

# Analysis of Neural Networks Used by Artificial Intelligence in the Energy Transition with Renewable Energies

Íñigo Manuel Iglesias-Sanfeliz Cubero <sup>1</sup>, Andrés Meana-Fernández <sup>1</sup>, Juan Carlos Ríos-Fernández <sup>1,\*</sup>, Thomas Ackermann <sup>2</sup> and Antonio José Gutiérrez-Trashorras <sup>1</sup>

<sup>1</sup> Department of Energy, University of Oviedo, 33203 Gijón, Spain;

uo224034@uniovi.es (Í.M.I.-S.C.); andresmf@uniovi.es (A.M.-F.); gutierrezantonio@uniovi.es (A.J.G.-T.)

<sup>2</sup> Department of Building Physics and Construction, University of Bielefeld, 32427 Minden, Germany;

thomas.ackermann@hsbi.de

\* Correspondence: riosjuan@uniovi.es

**Abstract:** Artificial neural networks (ANNs) have become key methods for achieving global climate goals. The aim of this review is to carry out a detailed analysis of the applications of ANNs to the energy transition all over the world. Thus, the applications of ANNs to renewable energies such as solar, wind, and tidal energy or for the prediction of greenhouse gas emissions were studied. This review was conducted through keyword searches and research of publishers and research platforms such as Science Direct, Research Gate, Google Scholar, IEEE Xplore, Taylor and Francis, and MDPI. The dates of the most recent research were 2018 for wind energy, 2022 for solar energy, 2021 for tidal energy, and 2021 for the prediction of greenhouse gas emissions. The results obtained were classified according to the type of structure and the architecture used, the inputs/outputs used, the region studied, the activation function used, and the algorithms used as the main methods for synthesizing the results. To carry out the present review, 96 investigations were used, and among them, the predominant structure was that of the multilayer perceptron, with Purelin and Sigmoid as the most used activation functions.

**Citation:** Iglesias-Sanfeliz Cubero, Í.M.; Meana-Fernández, A.; Ríos-Fernández, J.C.; Ackermann, T.; Gutiérrez-Trashorras, A.J. Analysis of Neural Networks Used by Artificial Intelligence in the Energy Transition with Renewable Energies. *Appl. Sci.* **2024**, *14*, 389. <https://doi.org/10.3390/app14010389>

Academic Editor: Frede Blaabjerg

Received: 14 November 2023

Revised: 7 December 2023

Accepted: 28 December 2023

Published: 31 December 2023



**Copyright:** © 2023 by the author. Licensee MDPI, Basel, Switzerland. This article is an open access article distributed under the terms and conditions of the Creative Commons Attribution (CC BY) license (<https://creativecommons.org/licenses/by/4.0/>).

## Highlights:

- The application of different types of RNA is very effective in the energy transition.
- ANNs are a very effective/useful tool in the fight against climate change.
- High capacity of ANNs to make predictions in different meteorological conditions.

**Keywords:** machine learning; artificial neural network; big data; energy transition

## 1. Introduction

Currently, the most accurate, most efficient, and most powerful machine for performing operations is the human brain, which can provide solutions to problems that PCs are not capable of solving. Researchers and scientists have developed artificial intelligence (AI) models to reproduce, to some extent, the processes that take place in the human brain [1]. Currently, AI is divided into different groups: artificial neural networks (ANNs) and different hybrid systems. Among them, ANNs are the best method as they are accurate, fast, and simple and have the ability to model a multivariate system [2].

The neural network (NN) concept has more than half a century of history; however, it is only in the last 20 years that the largest number of applications have been developed in the fields of defense, engineering, mathematics, economics, medicine, meteorology, and many others.

The history of neural networks dates to the 1940s. It was Warren McCulloch and Walter Pitts who first built a very simple neural network using electrical circuits [3]. Later, Donald Hebb proposed that neural pathways strengthen with each use, an important con-

cept in human learning [4]. Then, in the 1950s, Nathaniel Rochester of IBM Research Laboratories first attempted to simulate complex neural networks [5]. In 1959, Bernard Widrow and Marcian Hoff developed models called “ADALINE” and “MADALINE” [6,7]. After the publication of the book “Perceptrons” by Marvin Minsky and Seymour Papert in 1969, there was a period of slowdown in research. This book argued that the concept of a single perception approach to neural networks did not have an effective correlation in multilayer neural networks [8]. In the 1970s, two competing models emerged in the conception of neural networks, called symbolism and connectionism [9]. The controversy ended with the acceptance of the symbolic paradigm as the most viable line of research. In the early 1980s, however, connectionism resurfaced, based on Werbos’s 1974 studies. These studies made it possible to rapidly develop the formation of multilayer neural networks using the so-called “backpropagation” algorithm [10,11]. Since then, the field of neural networks has seen significant advances. Some of these advances were the introduction and development of max-pooling in three-dimensional data recognition [12]. On the other hand, advances included the development of deep learning and its application to a wide variety of fields such as renewable energy [12].

However, ANNs are not the only ones that learn by example. There are other methods, such as the following. Supervised learning: this method trains algorithms on the basis of sample input and output data labeled by humans [13]; deep learning: it uses neural networks to learn from the data and to improve performance by increasing the number of samples that are available during the learning process [14]; machine learning paradigms for unsupervised classification such as conceptual clustering [15], which is an unsupervised learning method that focuses on generating concept descriptions for the generated classes. Other machine learning paradigms that learn by example are semi-supervised learning [16], active learning [17], transfer learning [18], and online learning [19].

The data collection needed to train ANNs must be a sufficiently complete and consistent set of information [20]. The development of machine learning models requires historical data from several years, supplemented by information that is more recent. This information amounts to thousands of data points [20]. In the context of different energy transition scenarios and geographical locations, it is essential to ensure that the data collection is as complete, impartial, and representative as possible. This is achieved by managing diverse and reliable sources of information. Some of the most used sources are public repositories, data from official agencies and organizations, research centers, and geographic databases [21,22]. To ensure that the data are impartial, complete, and representative of all the energy transition scenarios analyzed, it is necessary to perform careful data selection and apply measures such as domain adaptation and data augmentation [23]. Model performance can also be improved, and training data can be augmented by using pretrained models in other domains [23]. The authors, based on the objective pursued and the exact geographical location, have analyzed all data obtained in the various studies, with latitude and longitude coordinates provided in many of them. Similarly, much of the data provided are based on measurements made by the authors themselves when using AI.

ANNs have gained momentum to the point where they have become popular and useful models for classification, clustering, recognition, and prediction in a wide variety of applications [24]. ANNs are increasingly being used for different applications due to their ability and effectiveness in solving different problems. They have proven to be very efficient when it is complex to cull through a mass of existing data, for example, in the evaluation of public transportation of people and goods [25], image recognition [26], medical analysis [27], efficiency analysis in nonlinear contexts, or to adjust production functions, among other applications [28,29].

ANN consists, in most cases, of an input layer, at least one hidden layer (in the case of a simplified model), an output layer, the weight, the connection biases, the activation function, and the sum node. The layers in turn are made up of several connected units (called neurons) [30], considered to be the fundamental building blocks for the correct

functioning of a neural network. The link between neurons is achieved by so-called connecting links [2]. The basic diagram of a neuron is shown in Figure 1 [31].

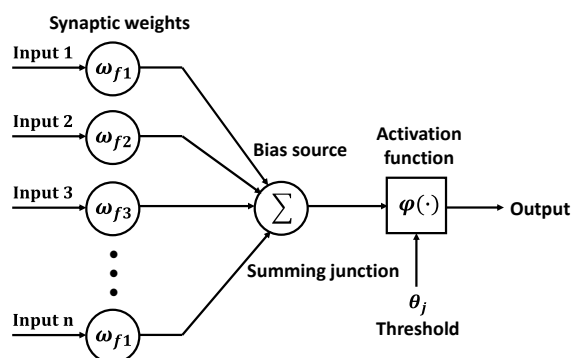


Figure 1. Schematic diagram of a neuron [31].

The main characteristic feature of ANNs compared to other approaches is their ability to learn by example. ANNs can be applied to any situation where there is a relationship between input and output variables [32]. The procedure for the learning process is what is known as a learning algorithm, the purpose of which is to alter the synaptic weights of the networks in order to achieve a previously set goal [33].

ANNs must be trained by feeding the network a set of quantified data to achieve the desired output using a pool of input data [34]. The learning process continues until the NN output matches the expected output [35]. The problem with ANN models lies precisely in overtraining, i.e., when the network capacity for training is too high or too many training iterations are allowed per network [36]. The degree of training accuracy obtained in the different applications where the ANN technique is used is very high, in the order of  $10^{-5}$  to complete the training processes [2]. NNs can be grouped into different categories depending on their structure [37]. This classification is shown in Figure 2. The most commonly used are single-layer feed-forward networks, multilayer feed-forward networks, radial basis networks, and dynamic (differential) or recurrent neural networks. Of these, single-layer power supply networks are the best known and most widely used. Single-layer power supply networks were the first and simplest networks devised. Information travels in only one direction: from input nodes, through hidden nodes, to output nodes. This type of NN can be designed based on different unities, and among them, the perceptron is the most famous and simplest example [38]. Rosenblatt created the perceptron in 1958, thanks to the creation of the training algorithm [39]. The perceptron is composed of a single neuron with adjustable synaptic weights and thresholds [40]. The most frequently used algorithm is the so-called backpropagation (BP) algorithm [41]. The BP algorithm consists of training and correcting the weights until the error function is below the desired tolerance limit [37].

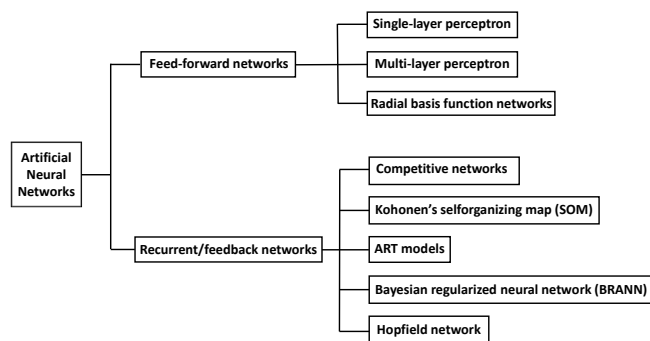


Figure 2. Artificial Neural Networks classification.

ANN models have proven to be a useful tool with great applications in different engineering systems. Unlike mathematical models, ANNs are able to adapt to real-world conditions [42]. Applications of NNs include forecasting [43,44], control [45], modeling [46], and pattern classification [47]. ANNs have been applied to different branches of engineering. In this work, given the wide variety of applications, it has been decided to classify them by energy type.

This article aims to provide a comprehensive review, as there is a lack of research in the literature that unifies in a single article the different ways of applying ANNs to the energy transition. It is of vital importance due to the increasingly frequent and significant environmental impacts and for the achievement of the United Nations (UN) Sustainable Development Goals, thus allowing researchers to know the state of the art so far on the different modalities of applying ANNs in the field of energy transition.

This review will focus on the contribution of renewable energies to the energy transition as the main contributors to mitigating the effects of climate change, as well as the applications of renewable energies to specific sectors such as buildings and transport. Finally, the different ways of using ANNs for the prediction of greenhouse gas emissions will be studied. The review has been carried out through the search and research of keywords in publishers and research platforms such as Science Direct, Research Gate, Google Scholar, IEEE Xplore, Taylor and Francis, and MDPI.

The study models had different applications in terms of scale. Some were designed to illuminate a single household, while others were designed for large-scale networks. The only difference lies in the size of the inputs provided by the authors to the neural networks. The models are highly versatile and have the potential to address energy planning needs and contribute to improvements in the energy transition. To ensure the reliability and robustness of neural networks in predicting or optimizing renewable energy systems, various methods and metrics can be used. Some of these methods are adversarial robustness evaluation [48]; robustness measurement and assessment (RoMA) [49]; extreme value theory approach [50]; and weight alterations [51]. These methods and metrics help evaluate the reliability and robustness of neural networks, especially in the context of adversarial attacks and environmental uncertainty.

The use of AI-powered neural networks in energy transition planning raises several ethical considerations. These considerations include decision making and accountability [52], as AI technology raises ethical questions related to decision making and accountability [53]; fairness and bias [54]; data privacy and security [55]; social responsibility [56], including job displacement and changes in economic structures; and environmental and climate implications [53], as the energy consumption of training large amounts of neural networks can be significant. By taking these ethical considerations into account, it would be possible to ensure that the use of AI-powered neural networks in energy transition planning is responsible, fair, and consistent with social values and environmental sustainability. Human experts are essential in the design, programming, and operation of AI to avoid unpredictable errors and to ensure that decisions made by AI are traceable [57]. In addition, AI development must adhere to principles such as accountability, transparency, verifiability, and predictability to serve society and fulfill human rights [57]. The concept of collaborative intelligence is important, where AI enhances human creativity and capabilities [58]. All of this achieves a responsible and ethical balance between the human experience and the capabilities of AI to serve the needs and preferences of society.

## 2. Applications of ANNs to Renewable Energies

This section details the different research carried out in the field of renewable energies and more specifically in wind, solar, and tidal energy. These three types of renewable energies have been selected as they are the ones that have the largest contributions to the national energy balances [59] as well as due to the greater abundance of works found.

### 2.1. Applications of ANNs for Wind Power and Speed Prediction

Within the renewable energy mix, wind energy is currently considered the most economical way to generate electricity. Recently, there has been new research into methods capable of predicting wind speed. This is of great importance due to the continuous growth of wind power generation worldwide [60]. For proper operation of wind farms, a constant stream of data about wind speed and wind direction is required. Artificial neural networks are an excellent method for short-, medium-, and long-term wind speed forecasting.

The following Table 1 summarizes the main research pieces found when performing the review. The studies have been classified according to the ANN structure, journal and region, input and outputs for the network, and the activation function employed.

**Table 1.** Uses of artificial neural networks for wind power and speed prediction.

Authors and Year	ANN Type and Structure	Journal	Country/Region	I/O Setting		Activation Function	Notes
				Input	Output		
1 [61]	Multilayer Perceptron (MLP) 3-4-1	Renewable Energy	Muppandal, India	Wind speed ( $W_s$ ), relative humidity (RH), generation hours	Energy output of wind farms	logsig (hidden layer) purelin (output layer)	Trained by BP algorithm Input data normalized to [0, 1]
2 [62]	ANN 4-X-2	Renewable Energy	Turkey	Longitude (lon), latitude (lat), altitude (A), measurement height	$W_s$ , related power	logsig (hidden and output layer)	Trained by BP algorithm Input and Output data normalized to [0, 1]
3 [63]	MLP 5-10-5-1	Renewable Energy	Turkey	$W_s$ , month (M)	$W_s$	logsig (hidden layer) purelin (output layer)	Resilient propagation (RP) algorithm was adopted
4 [64]	Radial Basis Function (RBF) 1-7-2	Renewable and Sustainable Energy Reviews	Iran	$W_s$	Proportional and integral (PI) gains	-	Use Gaussian function for hidden layer Gravitational search algorithm (GSA) is adopted Input data normalized to [0, 1]
5 [65]	MLP 3-(2-100)-24	Renewable Energy	Medina city, Saudi Arabia	Mean daily $W_s$	$W_s$ prediction of the next day	tansig (hidden layer) purelin (output layer)	Trained by Levenberg–Marquardt (LM) BP algorithm Compared and outperforms support vector machine (SVM) SVM used Gaussian kernel

								2000 days used for training and 728 days used for testing
6	[66]	MLP 6-7-5-1 MLP 4-7-5-1	Renewable and Sustainable Energy Reviews	Alberta, Canada	Wind power ( $W_p$ ) $W_{P1}(t-1)$ , $W_{P1}(t-2)$ , $W_{P1}(t-3)$ , $W_{P1}(t-4)$ , $W_{P1}(t-5)$ , $W_{P1}(t-6)$	Short-term forecasting of the $W_p$ time series	tansig (hidden layer) purelin (output layer)	Input data normalized to [-1, 1] Imperialist competitive algorithm (ICA), GA, and particle swarm optimization (PSO) are employed for training the neural network 1200 data used for training and 168 data used for testing
7	[67]	ANN 2-(16-32)-(16-32)-1	Renewable Energy	Coquimbo, Chile	$W_s$ , wind direction ( $W_d$ )	Turbine power	-	ADAM algorithm is adopted 103,308 data used for training and 52,560 data used for testing
8	[68]	RBF 2-3-1 MLP 2-4-1 ADALINE 2-4-1	Applied Energy	North Dakota, USA	Mean hourly $W_s$	Forecast value of next hourly average $W_s$	-	Trained by LM algorithm 5000 data used for training and 120 data used for testing
9	[69]	MLP 5-5-3	Renewable Energy	Guadeloupean archipelago, French West Indies	$W_s$ , 30 min moving average speed	$W_p(t+kt)$	tansig (hidden layer) purelin (output layer)	Bayesian regularized (BR)
10	[70]	ANN 7-20-1	Renewable Energy	China	Actual $W_s$ , $W_p$	$W_s$	-	Trained by BP algorithm
11	[71]	MLP 6-7-1	Renewable Energy	Albacete, Spain	$W_{sp1}$ , $W_{sp2}$ , temperature (T) $T_{p2}$ , solar cycle <sub>1</sub> , solar cycle <sub>2</sub> , $W_{dp1}$	$W_s$ forecast (48 h later)	-	LM algorithm is adopted
12	[72]	ANN 3-3-1 ANN 3-2-X ANN 3-1 ANN	Renewable Energy	Oaxaca, México	Previous values of hourly $W_s$	Current value of $W_s$	-	550 data used for training and 194 data used for testing

2-1								
13	[73]	ANN -	Renewable Energy	Basque Country, Spain	$W_s$ data in the last 3 h	$W_s$ in 1 h	sigmoid (output layer)	Trained by BP algorithm
14	[74]	MLP X-8-X	Renewable Energy	Rostamabad, Iran	Standard deviation, average, slope	$W_s(k+1), \dots$ $W_s(k+2)$ , $W_s(k+1)$	-	Trained by BP algorithm 672 patterns used for training
15	[75]	MLP 5-3-3-1	Communications in Nonlinear Science and Numerical Simulation	Italy	$W_s$ , RH, generation hours, T, maintenance hours	Total wind energy	tansig (first hidden layer) sigmoid (second hidden layer) purelin (output layer)	Trained by BP algorithm
16	[76]	MLP 6-25-1	Renewable Energy	Himachal Pradesh, India	Average temperature ( $T_{AVG}$ ), maximum temperature ( $T_{max}$ ), minimum temperature (ax), air pressure ( $P_{air}$ ), solar irradiance (G), A	Average daily $W_s$ for 11 H.P. locations	-	Trained by LM algorithm Scaled conjugate gradient (SCG) algorithm is adopted Input and target data are normalized to [-1, 1] 60% data used for training, 20% used for testing, and 20% used for validation
17	[77]	MLP 4-15-15-1	Applied Energy	Nigeria	lat, lon, A, M	Mean monthly $W_s$	tansig (hidden layers) purelin (output layer)	SCG and LM algorithms are adopted Input and target data normalized to [-1, 1]
18	[78]	MLP 14-15-1	WSEAS Transactions on Systems	Portugal	Average hourly values of $W_s$	Average hourly $W_s$	-	Trained BP algorithm 87.75% patterns used for training, 9.75% used for validation, and 2.5% used for testing
19	[79]	MLP 5-6-6-6-2	-	Cyprus	M, mean monthly values of $W_s$ at two levels (2 and 7 m)	Mean monthly values of $W_s$ of a third station	tansig (hidden layer) logsig (output layer)	Trained by BP algorithm 90% patterns used for training and 10% patterns used for testing
20	[80]	MLP 9-10-1	Energy	Marmara, Turkey	9 stations $W_s$	$W_s$	-	Trained by BP algorithm

Conversion and Management								
21	[81]	MLP 4-8-1	Theoretical and Applied Climatology	Tabriz, Azerbaijan, Iran	$P_{air}$ , air temperature ( $T_{air}$ ), RH, precipitation	Monthly $W_s$	logsig (hidden layer) purelin (output layer)	Trained by LM algorithm Input and output data normalized to [0, 1] 75% of data used for training and 25% used for testing
22	[82]	MLP 31-63-31	Knowledge-Based Systems	Minqin, China	Historical daily average $W_s$ during March previous year	Daily average $W_s$ during March target year	tansig (hidden layer) logsig (output layer)	Trained by BP algorithm
23	[83]	MLP X-25-1	2014 4th IEEE International Conference on Information Science and Technology	Colorado, USA	T, RH, $W_d$ , wind gust, pressure (P), historical $W_s$	$W_s$	tansig (hidden layer)	Trained by BP with momentum 1000 input/output pairs used for training and 200 input/output pairs used for testing

The applications have different characteristics in several aspects, such as the ANN structure, the input data, the activation function used, and the training algorithm. As can be seen from the literature, various studies on wind speed prediction have been carried out for more than twenty years in different parts of the world, most of them located in Turkey, India, China, or Iran.

The main characteristics of the networks studied are detailed below.

- ANN type: from the 23 references analyzed, the MLP network has been used in 17 of them, followed by the RBF in two of them. Five of them did not specify the type of ANN used.
- Structure of the ANN: the predominant type is simple with one hidden layer (70%) and the rest with two hidden layers (26%) with the exception of the investigation of [41], which uses three hidden layers. The number of neurons in the hidden layer is usually around 15, while in other cases more than 63 are selected [44].
- Amount of data: the percentage of research that makes use of data for validation is 8.69%.
- I/O configuration: the inputs to the models usually take in situ measured features such as past wind speeds, temperature, relative humidity, altitude, month, or pressure.
- Activation function: only 13 of the 23 cases detail the activation function used. In the hidden layer, linear functions are used, with tansig and logsig being the most commonly used, while in the output layer, linear functions of the purelin type are adopted.

Figure 3 details the most common inputs and outputs used by ANNs in wind power and wind speed prediction and the operating scheme.



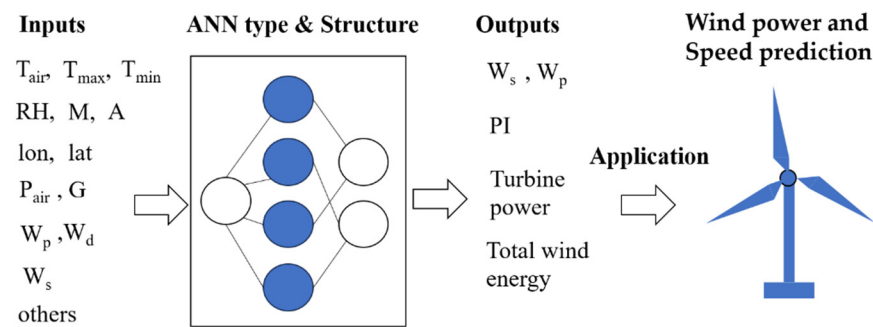


**Figure 3.** Inputs and outputs in ANNs applied to wind energy and wind speed prediction.

ANNs are highly recommended for predicting wind speed and power generation for several reasons, including self-learning, low error, and high efficiency predictability [84].

## 2.2. Applications of ANNs for Solar Energy Systems

Within solar energy, the ANN technique has proven to be an alternative to conventional methods, providing great benefits in terms of precision, performance, and modeling. The study indicates that the advantage of ANN techniques over conventional techniques is that they do not require knowledge of internal system parameters, require less computational effort, and offer robust outputs to multivariate problems. NN modeling requires data representing the history, the current performance of the real system, and a correct selection of a NN model. Mellit et al. [85] conducted an overview of the different AI techniques for sizing PV systems. The research shows that one of the advantages of AI in modeling PV systems is that it allows good optimization in isolated areas, where meteorological data are not always available. Mellit and Kalogiriu [86] have applied AI techniques to model, predict, simulate, optimize, and control photovoltaic systems.

The applications of ANNs to solar energy go beyond that, as there is also research such as the one carried out in [42], in which the application of the ANN technique seeks to optimize and predict the performance of the different devices involved in a solar energy system such as solar collectors, heat pumps, or solar air. The research shows how the application of ANNs can save time and reduce the financial costs of the system since it is not necessary to carry out so many experimental tests to determine the relationship between the input and output variables. Another application of ANNs is shown in the research of [87], where the performance of solar collectors is predicted, thus improving the efficiency of the system as a whole. The developed model also showed advantages over conventional computational methods in terms of calculation and prediction time.

Solar radiation data are very important because in most cases they are not available due to the lack of a meteorological station. It is therefore necessary to have techniques to accurately predict solar radiation. ANNs are the solution to the problems of conventional methods [88].

Different ANN models have been applied for solar irradiance prediction, such as the MLP neural network, the RBF neural network, or the general regression neural network (GRNN). The different studies have been classified, taking into account different factors such as network structure and type, input/output configuration, or the activation function and tuning algorithm employed, as is shown in Table 2.

**Table 2.** Uses of artificial neural networks for solar energy prediction.

Authors and Year	ANN Type and Structure	Journal	Country/Region	I/O Setting		Activation Function	Notes
				Input	Output		
1 [89]	RBF 6-11-24 RBF 6-15-24	Solar Energy	Huazhong, China	$G(t+1)$ , $W_s(t+1)$ , $T_{air}(t+1)$ , $RH(t+1)$ , $t$ , power ( $P_w$ ) ( $t$ )	$P_{w1}(t+1)$ , $P_{w2}(t+1)$ , ... $P_{w24}(t+1)$	-	k-fold (validation) Input and output data normalized to [0, 1]
2 [90]	MLP 2-3-1	Renewable Energy	Jaen, Spain	$G$ , module cell temperature ( $T_c$ )	$G$ , ambient temperature ( $T_a$ )	-	Trained by LM BP algorithm
3 [91]	MLP 3-3-1 MLP 4-3-1	Energy	Corsica Island, France Bastia  Ajaccio	$RH$ , sunshine duration ( $S$ ), nebulosity ( $Y$ )  $Y, S, P$ , differential pressure ( $DGP$ )	Global radiation ( $GR$ )	tansig (hidden layer) purelin (output layer)	Trained by LM algorithm Input data normalized to [-1, 1] 80% data used for training, 10% for validation, and 10% used for testing
4 [92]	MLP 8-3-1	Solar Energy	Ajaccio, Corsica Island, France	Clearness index ( $K_T$ ) $K_{Tt-1}, K_{Tt-2}$ , $K_{Tt-3}, K_{Tt-4}$ , $K_{Tt-5}, K_{Tt-6}$ , $K_{Tt-7}, K_{Tt-8}$	Daily global solar radiation ( $GSR$ )	purelin (output layer)	Trained by LM algorithm Use Gaussian function for hidden layer Input data normalized to [0, 1] 80% data used for training, 10% for validation, and 10% used for testing
5 [93]	MLP 3-11-17-24	Solar Energy	Trieste, Italia	$G, T_{air}$ , hour or day ( $t$ )	$G_1(t+1), G_2$ ( $t+1$ ), ..., $G_{24}$ ( $t+1$ )	-	Trained by LM BP Algorithm k-fold validation Input and output data normalized to [-1, 1]
6 [94]	RBFN (2-3-4)- (4-5-7)-1 MLP (2-3-4)- (2-3-5)-1	Energy	Al-Medina, Saudi Arabia	$T_{air}, S, RH, t$	Daily global solar radiation ( $G_D$ )	-	1460 data used for training and 365 data used for testing
7 [95]	MLP 6-5-1	Applied Energy	Turkey	lat, lon, $A$ , $M, S, T$	$G$	logsig (hidden layer)	Trained by BP algorithm SCG, Pola-Ribiere conjugate gradient (CGP), and LM

								algorithms are adopted Input and output data normalized to [-1, 1]
8	[96]	MLP 3-20-1	Renewable and Sustainable Energy Reviews	Morocco	lon, lat, A	Mean annual and monthly G	-	Trained by BP algorithm Input and output data normalized to [0, 1]
9	[97]	MLP 2-36-1 MLP 3-20-1	Energy Sources, Part A: Recovery, Utilization, and Environmental Effects	Abha, Saudi Arabia	T <sub>air</sub> , RH, hour or day (t)	Diffuse solar radiation (DSR)	logsig (hidden layer)	Trained by BP algorithm 1462 days used for training and 250 days used for testing
10	[98]	MLP 5-8-1	Expert Systems with Applications	Anatolia, Turkey	lat, lon, A, S, average cloudiness	G	tansig (hidden layer) purelin (output layer)	Trained by BP algorithm
11	[99]	MLP 7-5-1	Applied Energy	Nigeria	lat, lon, A, M, S, T, RH	G	tansig (hidden layer) purelin (output layer)	SCG and LM algorithms are adopted Input data normalized to [-1, 1] 11,700 datasets used for training and 5850 datasets used for validation and testing
12	[100]	MLP 4-X-1	International Journal of Photoenergy	Malaysia	lat, lon, day or hour (t), S	K <sub>T</sub>	logsig (hidden layer)	Trained by BP algorithm
13	[101]	MLP 4-4-1	International Journal of Computer Applications	India	lat, lon, S, A	G	tansig (hidden layer) purelin (output layer)	LM algorithm is adopted
14	[102]	MLP 5-40-1	Energy	Egypt	GSR, like long-wave atmospheric emission, T <sub>air</sub> , RH, P	Diffuse fraction (K <sub>D</sub> )	sigmoid (output layer)	Trained by BP algorithm
15	[103]	MLP 7-15-1	Solar Energy	Jaen, Spain	t (day), t (hour), K <sub>T</sub> , hourly clearness	Solar radiation maps	-	Trained by BP algorithm (with momentum and random presentations)

						index ( $k_t$ ) $k_{t-1}, k_{t-2}, k_{t-3}, S$		Input data normalized to [0, 1]
16	[104]	MLP 6-X-1	Solar Energy	Helwan, Egypt	$W_d, W_s, T_a, RH,$ cloudiness, water vapor	G	sigmoid (output layer)	Trained by LM BP algorithm Input data normalized to [0, 1]
17	[105]	MLP 2-X-1 MLP 3-X-1 MLP 3-X-X-1	Solar Energy	Athalassa, Cyprus	S, theoretical sunshine duration ( $S_{0d}$ ), M, $T_{max}$	$G_D$	tansig (hidden layer)	Trained by BP algorithm 90% data used for training and 10% used for testing
18	[106]	MLP 7-9-1	Renewable Energy	India	lat, lon, A, M, S, rainfall ratio, RH	$K_T$	tansig (hidden layer) purelin (output layer)	Trained by BP algorithm
19	[107]	MLP 2-5-1	Energy Policy	China	$K_t, S$ (%)	Monthly mean daily $K_D$	tansig (hidden layer) purelin (output layer)	Trained by BP algorithm TRAINLM algorithm is adopted Input and output data normalized to [0, 1]
20	[108]	MLP 6-15-1	Solar Energy	Uganda	S, $T_{max}$ , Total Cloud Cover (TCC), lat, lon, A	Monthly average daily GSR on a horizontal surface	tansig (hidden layer) purelin (output layer)	Trained by LM BP algorithm Input data normalized to [-1, 1]
21	[109]	MLP 6-6-1	Applied Energy	Turkey	lat, lon, A, M, DSR, mean beam radiation	G	logsig (hidden layer) purelin (output layer)	SCG and RP algorithms are adopted
22	[110]	GRNN 6-1.0-1	Energy	Turkey	lat, lon, A, surface emissivity ( $\epsilon_4$ ), surface emissivity ( $\epsilon_5$ ), land surface temperature	G	-	-
23	[111]	MLP 7-4-1	Energy Conversion and Management	Iran	$T_{max}, T_{min}, RH, VP,$ total precipitation, $n, W_s, S$	GSR	logsig (hidden layer) purelin (output layer)	Trained by BP algorithm 65 months used for training and 7 months used for testing

24	[112]	ANN 6-6-1	Applied Energy	Turkey	lat, lon, A, M, S, T	G	logsig (hidden layer)	SCG, CGP, and LM algorithms are adopted Trained by BP algorithm Input and output data normalized to [-1, 1]
25	[113]	MLP 3-6-1	Renewable Energy	Khuzestan, Iran	T <sub>max</sub> , T <sub>min</sub> , extra- terrestrial radiation (R <sub>a</sub> )	GSR	logsig (hidden layer)	Trained by LM BP algorithm Input data normalized to [0, 1] 70% data used for training and 30% patterns used for testing
26	[114]	MLP 5-3-1	Energy Procedia	Bechar, Algeria	M, t (day), t (hour), T, RH	GSR	tansig (hidden layer) purelin (output layer)	Trained by LM BP algorithm 81% data used for training and 19% used for testing
27	[115]	MLP 9-11-1	Renewable and Sustainable Energy Reviews	Republic of Indonesia	T, RH, S, W <sub>s</sub> , precipitatio n, lon, lat, A, M	GSR	-	Trained by BP algorithm
28	[116]	RBF 4-50-2	Energy Sources, Part A: Recovery, Utilization, and Environment al Effects	Saudi Arabia	T <sub>a</sub> , RH, GSR, t	DSR, direct normal radiation (DNR)	-	Use Gaussian function for hidden layer 1460 values used for training and 365 values used for testing
29	[117]	MLP 8-15-1	Renewable Energy	Sultanate of Oman	Location (L), M, P, T, VP, RH, W <sub>s</sub> , S	GR	-	Trained by BP algorithm

In contrast to the previous case, there is more literature available and the existing research from 1998 to 2012 has been collected. Most of the studies focus on countries that enjoy strong and prolonged hot climates such as the countries bordering the Mediterranean Sea as well as Saudi Arabia and China. As in the previous section and as mentioned at the beginning, the different applications are analyzed. The main characteristics of the networks studied are detailed below.

- ANN type: in most of the investigations, the MLP network has been used (24 out of 29 cases) followed by the RBF.
- Structure of the ANN: most studies use simple structures with a single hidden layer (96%), and the remaining with two hidden layers. The number of neurons in the hidden layer is usually in the order of 10, reaching 50 neurons in the research of [116]. In some cases, the number of neurons in the hidden layer is not specified, as in [105] and [104].

- Amount of data: the percentage of research that make use of data for validation is 6.9%.
- I/O configuration: altitude, latitude, longitude, relative humidity, or month of the year are used as the most common inputs.
- Activation function: only 19 of the 29 investigations detail the activation function used. In the hidden layer, linear functions are used, with tansig and logsig being the most commonly used, while in the output layer, linear functions of the purelin type are adopted.

Figure 4 details the most common inputs and outputs used by ANNs in solar energy prediction and the operating scheme.

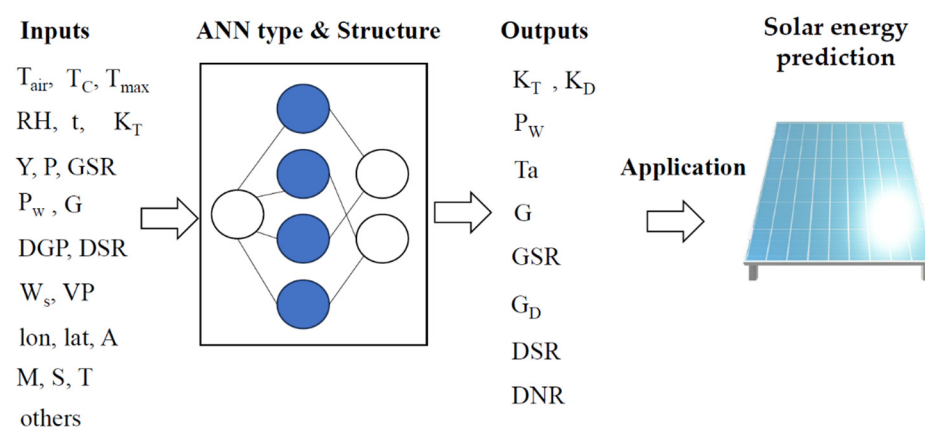


Figure 4. Inputs and outputs in ANNs applied to solar energy systems.

### 2.3. Applications of ANNs for Wave Prediction

Tidal energy, like other renewable energies, is fundamental to achieving the European climate targets for 2030 and 2050. Recently, the use of NNs for wave height (H) and period prediction has gained importance. ANNs have also been applied in different fields of ocean, coastal, and environmental engineering [118]. The following table summarizes the main research pieces found when performing the review. The studies have been classified according to the ANN structure, journal and region, input and outputs for the network, and the activation function employed. The following Table 3 shows the H predictions.

Table 3. Uses of artificial neural networks for wave height prediction.

Authors and Year	ANN Type and Structure	Journal	Country/Region	I/O Setting		Activation Function	Notes
				Input	Output		
1 [119]	ANN 28-15-4 28-9-4 28-4-4 28-7-4	Journal of Atmospheric and Oceanic Technology	Gulf of Maine, Gulf of Alaska, Gulf of Mexico	7 days of significant H	6, 12, 18, 24 h forecast	logsig (hidden and output layer)	Input data normalized to [0, 1] Conjugate gradient algorithm with Fletcher–Reeves is adopted
2 [120]	MLP 3-5-5-2	Ocean Engineering	Bombay, India	Deep water wave height (H <sub>o</sub> ), wave energy period (T <sub>e</sub> )	Breaking wave height (H <sub>b</sub> ), water depth at the time of	sigmoid (output layer)	Trained by BP algorithm Input and output data normalized to [0, 1]

						breaking (db)		
						H and zero-up-crossing		
3	[121]	MLP 48-97-24	Ocean Engineering	Ireland	48 h history wave parameters	peak wave period ( $T_p$ ) over hourly intervals from 1 h to 24 h	logsig (hidden layer) purelin (output layer)	Trained by resilient BP algorithm
4	[122]	MLP 6-5-1	Proceedings of the Institution of Civil Engineers-Maritime Engineering	Anzali, Iran	$H, T_p$	Energy flux ( $F_e$ ) over horizon of 1 to 12 h	sigmoid (output layer)	Conjugate gradient algorithm is adopted 80% data used for training and 20% used for testing
5	[123]	MLP 2-4-3 MLP 4-4-4	Ocean Engineering	Karwar, India	$W_s$	3-hourly values of H and average cross-period	-	Trained by BP algorithm 80% data used for training and 20% data used for testing
6	[124]	Deep Neural Network (DNN) 6-64-32-32-1	Ocean Engineering	Pacific and Atlantic coasts and the Gulf of Mexico	$H, T_e, F_e$ , weighted average period, $T_p$ , $W_s, W_d$	$F_e, T_e, H$	-	SCG BP algorithm is adopted Input data normalized to [0, 1] 75% data used for training and 25% data used for testing
7	[125]	MLP 3-300-300-2	Ocean Engineering	Lake Michigan, United States of America	Wind field, db, ice coverage	$H, T_e$	ReLU (hidden layer)	Stochastic gradient-based algorithm is adopted 80% data used for training and 20% data used for testing
8	[126]	MLP 1-x-1	Marine Structures	Goa, India	H	$F_e$	sigmoid (output layer)	Trained by BP cascade correlation algorithms 80% patterns used for training and 20% patterns used for testing
9	[127]	MLP 6-5-1	Ocean Engineering	Persian Gulf	$H_t, H_{t-1}, H_{t-2}, U_t \cos(\Phi t - \theta), U_{t-1} \cos(\Phi t - 1 - \theta t), U_{t-2} \cos(\Phi t - 2 - \theta t)$	H for the next 3,6,12,24 h	sigmoid (output layer)	Conjugate gradient and LM algorithms are adopted 80% data used for training and 20% data used for testing
10	[128]	MLP 3-4-4-1	Applied Soft	Spain	$H, T_e, \theta_m$	$F_e$	tansig	Trained by BP algorithm

			Computing				(hidden layer) purelin (output layer)	67% data used for training and 33% data used for testing
11	[129]	MLP 3-3-1	Ocean Engineering	Lake Superior, USA	$W_s$ , weather station index (W)	H	sigmoid (hidden and output layer)	Trained by BP algorithm Input and output data normalized to [-1, 1] Compared with SVM, Bayesian networks, and adaptive neuro-fuzzy inference system (ANFIS) 345 patterns used for training and 54 patterns used for testing
12	[130]	MLP 5-2-1	Renewable Energy	Brazil	Wind shear velocity ( $U$ ) $U_1, U_2, U_n$ , $Y(t-1)$ , $Y(t-i)$	Wave energy potential	tansig (hidden layer) purelin (output layer)	Trained by LM BP algorithm 90% data used for training and 10% data used for testing
13	[131]	MLP X-15-1	Applied Ocean Research	Canary Islands, Spain	$H, T_p$	Predict $F_e$	tansig (hidden layer) purelin (output layer)	Gradient descent with momentum and BP algorithm are adopted 89% data used for training and 11% data used for testing Input and output data normalized to [-1, 1]
14	[132]	MLP 4-4-1	Applied Ocean Research	India	H values of the preceding 3, 6, 12, and 24th hour	H subsequent 3,6,12 and 24th hour	-	Trained by LM BP algorithm 60% data used for training and 40% data used for testing
15	[133]	RBF 21-13-1 MLP 21-9-1	Marine Structures	India	$H_{(1-21)}$	$H(SW3)$	-	Use Gaussian function for hidden layer BP, SCG, conjugate gradient Powell–Beale (CGB), Broyden–Fletcher–Goldfarb (BFG), and LM algorithms are adopted 80% data used for training and 20% data used for testing
16	[134]	MLP 8-4-1	Ocean Engineering	Taiwan	Significant wave	$H_{1/3}$ (station C)	sigmoid	Trained by BP algorithm



		MLP 2-2-1			height ( $H_{1/3}$ ), highest one-tenth wave height ( $H_{1/10}$ ), highest wave height ( $H_{max}$ ), mean wave height ( $H_{mean}$ ) (stations A and B)		(output layer)	Input data normalized to [0, 1]
17	[135]	MLP 2-5-1	Marine Structures	Yanam, India	$H_t, H_{t-1}$	$H_{t+1}$	-	Trained by BP algorithm Conjugate gradient and cascade correlation algorithms are adopted 80% data used for training and 20% data used for testing
18	[136]	ANN 9-1-1 ANN 4-1-1 ANN 9-8-1 ANN 9-1-1	Applied Ocean Research	Ratnagiri, Pondicherry, Gopalpur, Kollam, India	$t - 24,$ $t - 21,$ $t - 18,$ $t - 15,$ $t - 12, t - 9,$ $t - 6, t - 3$	$t + 24$ (24 h ahead predicted error)	logsig (hidden layer) purelin (output layer)	Trained by LM algorithm Input data normalized to [0, 1] 70% data used for training and 15% used for validation and testing
19	[137]	MLP 4-9-3 MLP 4-7-1 MLP 2-5-1 MLP 4-8-1	Applied Ocean Research	Lake Ontario, Canada/USA	$W_s, W_d,$ fetch length, wind duration	$H, T_p,$ (wave direction) $\Theta$	tansig/ sigmoid (hidden layer) purelin (output layer)	Trained by BP algorithm 10-fold cross- validation used Input data normalized to [0, 1] 611 data used for training and 326 data used for testing
20	[138]	MLP 1-3-1	Ocean Engineering	Lake Superior, Canada/USA	$W_s$	$H$	sigmoid (transfer function)	Compared and outperforms with model tree 4045 data used for training and 3259 data used for testing

While it is true that studies appear in the literature since 2001, unlike the two previous cases, there has been an increase in the number of studies carried out in recent years.

Most of the research is concentrated in India, Canada, and the United States and applies to both lakes and the open sea. The main characteristics of the networks studied are detailed below.

- ANN type: as in previous cases, the MLP has been the structure chosen by most researchers (17 out of 20 cases). Research using the DNN [124] and RBF [133] has also been found.
- Structure of the ANN: most of the studies analyzed use simple structures with a single hidden layer. Research has also been found that uses two hidden layers or even the research of [124], which uses three. The number of neurons in the hidden layer is usually in the order of 10, reaching 300 neurons in the research of [125].
- Amount of data: in most research, the volume of data is in the order of hundreds or thousands. Normally, a major part of the data is used for training, with the remainder applied to testing. The percentage of studies that make use of data for validation is 5%.
- I/O configuration: temperature, wind speed, wind direction, and historical wave data are normally used as inputs. Outputs predict wave heights from one hour to 24 hours in advance.
- Activation function: the activation function is specified in 15 out of the 20 research. In the hidden layer, linear functions are used, with tansig and logsig being the most commonly used, while in the output layer, linear functions of the purelin and sigmoid types are adopted.

As a summary of all the previous sections, in the case of renewable energies, the predominant structure chosen is the multilayer perceptron structure with one or two hidden layers, because it may act as a universal function approximator. In addition, together with the backpropagation algorithm, it is able to learn any type of continuous function between a set of input and output variables.

Figure 5 details the most common inputs and outputs used by ANNs in wave height prediction and the operating scheme.

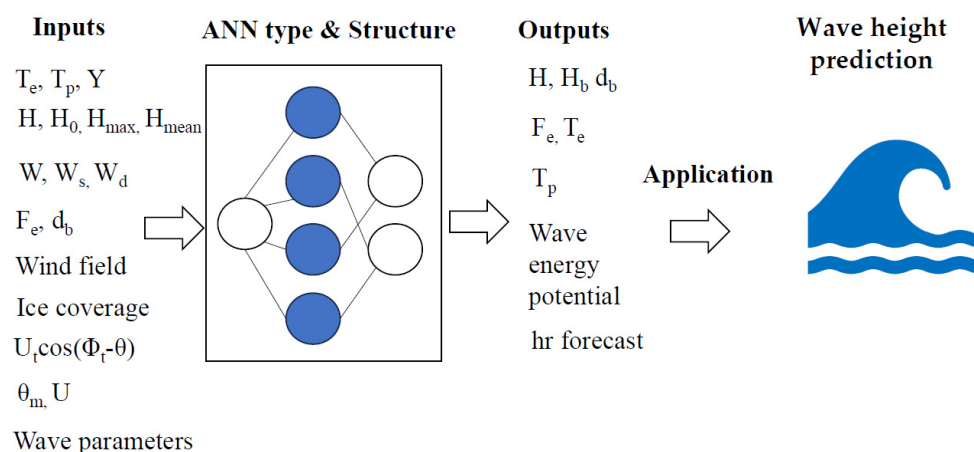


**Figure 5.** Inputs and outputs in ANNs applied to wave prediction.

### 3. Applications of ANNs for GHG Prediction

Traditionally, different techniques have been used to estimate greenhouse gas (GHG) emissions, such as the synergies and interactions model of air pollution and greenhouse gases [139]. The technique of ANNs is different from the GAINS (greenhouse gas and air pollution interactions and synergies) model in that ANNs are less complex, require a smaller amount of input data, and the inputs are undetermined [140]. The different research in the literature from 1996 to 2021 is detailed in Table 4.

**Table 4.** Uses of artificial neural networks for GHG prediction.

Authors and Year	ANN Type and Structure	Journal	Country/Region	I/O Setting		Activation Function	Notes
				Input	Output		
1 [141]	MLP 12-8-2	Agricultural Systems	Iran	Machinery, human labor, diesel fuel, pesticide, nitrogen (N), phosphate (P <sub>2</sub> O <sub>5</sub> ), potassium (K <sub>2</sub> O), farmyard manure (FYM), water for irrigation, electricity, seed, farm size	Energy, GHG emission	tansig (hidden layer)	Trained by BP algorithm 60% data used for training, 25% data used for cross-validation, and 15% data used for testing
2 [142]	MLP 9-4-1	Environmental Pollution	Texas, USA	Dummy variable, ozone (O <sub>3</sub> ) level at 9:00 am, carbon dioxide (CO <sub>2</sub> ), nitric oxide (NO), nitrogen dioxide (NO <sub>2</sub> ), oxide of nitrogen (NO <sub>x</sub> ), W <sub>s</sub> , W <sub>d</sub> , T <sub>max</sub>	Daily maximum O <sub>3</sub> level	tansig (hidden layer)	Trained by BP algorithm
3 [143]	MLP 6-20-20-2	Atmospheric Environment	London, UK	Low cloud amount (LOW), base of lowest cloud (BASE), UKMO, visibility (VIS), T <sub>d</sub> , VP, W <sub>s</sub>	NO <sub>x</sub> , NO <sub>2</sub>	tansig (hidden layer) identify (output layer)	SCG algorithm is adopted Input and output data normalized to [-1, 1]
4 [144]	MLP 3-x-1	Atmospheric Environment	Santiago, Chile	W <sub>s</sub> (t), W <sub>d</sub> (t), G (t), G (t - 1), G (t - 2), G (t - 3), SO <sub>2</sub> (t),	O <sub>3,t</sub> , T <sub>t+1</sub> , T <sub>t</sub>	O <sub>3,t+1</sub>	sigmoid (output layer) Direct algorithm or series-parallel was used
5 [145]	MLP 10-25-1 MLP 10-11-1	Neural Computing Y Applications	Ravenna, Italy	W <sub>s</sub> (t), W <sub>d</sub> (t), G (t), G (t - 1), G (t - 2), G (t - 3), SO <sub>2</sub> (t),	Sulphur dioxide (SO <sub>2</sub> ) (t + 1)	tansig (output layer)	BR SCG algorithm is adopted 20% data used for testing

					SO <sub>2</sub> (t - 1), SO <sub>2</sub> (t - 2), SO <sub>2</sub> (t - 3)		logsig (output layer)	
6	[146]	Elman NN 4-13-3	Environmental Modelling Y Software	Delhi, India	W <sub>s</sub> , T, RH, W <sub>d</sub>	Predict SO <sub>2</sub> concentratio n	sigmoid (hidden layer) purelin (output layer)	Trained by LM algorithm
7	[147]	MLP 5-X-1 MLP 9-X-1	Environmental Modelling Y Software	Bilbao, Spain	W <sub>s</sub> , W <sub>d</sub> , T, RH, P, G, thermal gradient, O <sub>3</sub> , NO <sub>2</sub> , number of vehicles, occupation percentage, velocity sin (2πt/24), cos (2πt/24), sin (2πt/7), cos (2πt/7), NO <sub>2</sub> (t + k), O <sub>3</sub> (t + k)	O <sub>3</sub> (t + k) NO <sub>2</sub> (t + k) (k = 1,...8)	tansig (hidden layer) purelin (output layer)	SCG algorithm is adopted 85% data used for training and 15% data used for validation and testing
8	[148]	ANN 13-25-1	Advances in Environmental Research	Kuwait	Mon-methane hydrocarbons, carbon monoxide (CO), methane (CH <sub>4</sub> ), CO <sub>2</sub> , SO <sub>2</sub> , NO, NO <sub>2</sub> , T, RH, suspended dust, solar energy, W <sub>d</sub> , W <sub>s</sub>	O <sub>3</sub> concentratio n	logsig (hidden layer)	Trained by BP algorithm with momentum Input data normalized to [0, 1] 90% data used for training and 10% data used for testing
9	[149]	GRNN (7-13)-154-1	Science of The Total Environment	EU-27	Gross domestic product (GDP), gross inland energy consumption (GIEC), incineration of wood...	Annual (particle matter) PM <sub>10</sub> emission	-	GA was used Input data normalized per capita 84% data used for training and 16% data used for validation
10	[150]	MLP 7-4-1	Atmospheric Environment	Belgium	PM <sub>10</sub> , boundary layer height (BLH), W <sub>s</sub> , T, cloud, W <sub>d</sub> , t	Daily average PM <sub>10 day1</sub>	-	Trained by BP algorithm

11	[151]	MLP 4-5-10-1	Energy	Europe	Intake pressure, m, fuel consumption, engine power	Raw emissions NOx	sigmoid (hidden layers) purelin (output layer)	Trained by BP algorithm Input data normalized to [-1, 1] 70% data used for training and 30% data used for testing
12	[152]	MLP 4-13-5	Applied Energy	Tamil Nadu, India	Pre-injection timing (PrIT), main injection timing (MIT), post-injection timing (PIT), test fuels	CO, CO <sub>2</sub> , unburned hydrocarbon (UBHC), NO, smoke	sigmoid (hidden layer)	Trained by LM BP algorithm Input data normalized to [-1, 1] 70% data used for training, 15% data used for validation, and 15% data used for testing
13	[153]	MLP 3-(13-7)-1	Applied Energy	-	Injection pressure, engine speed, throttle position (TP)	NO <sub>x</sub> , CO <sub>2</sub> , SO <sub>2</sub>	logsig (hidden layer)	Trained by BP algorithm SCG, CGP, and LM algorithms are adopted Input and output data normalized to [0, 1]
14	[154]	MLP 2-20-9	Applied Energy	Iran	Engine speed, ethanol gasoline blend	Brake power, torque, brake-specific fuel consumption (BSFC), brake thermal efficiency (BTh), volumetric efficiency ( $\eta_v$ ) CO, CO <sub>2</sub> , hydrocarbons (HC), NO <sub>x</sub>	sigmoid (hidden layer) purelin (output layer)	Trained by BP algorithm 70% data used for training and 30% data used for testing
15	[155]	MLP 4-15-5	Applied Thermal Engineering	-	Lower heating value (LHV), engine torque, engine speed, air inlet temperature	BSFC, BTh, CO, HC, exhaust gas temperature (EGT)	sigmoid (hidden layer)	Trained by LM BP algorithm 70% data used for training and 30% data used for testing
16	[156]	MLP 4-22-3	Applied Energy	-	Load, blend %, compression ratio, injection timing	NO <sub>x</sub> , smoke, UBHC	sigmoid (hidden layer) purelin (output layer)	Trained by BP algorithm Input data normalized to [-1, 1] 70% data used for

								training, 15% data used for validation, and 15% data used for testing
17	[157]	MLP 4-(7-60)-1	Applied Soft Computing	Iran	Engine speed, intake air temperature, mass fuel, brake power	NO <sub>x</sub>	logsig (hidden and output layer)	CGP, CGB, GDM, GD, and LM algorithms are adopted Output data normalized to [0, 1] 90% patterns used for training and 10% patterns used for testing
18	[158]	MLP 6-14-1	Proceedings of the 28th International Symposium on Forecasting	Italy	Oil, solid fuel, electricity, natural gas, population, GDP	CO <sub>2</sub>	logsig (output layer)	Trained by BP algorithm Input normalized to [0, 1]
19	[159]	MLP 6-9-1	Journal of Cleaner Production	Turkey	Year, coal, liquid fuels, natural gas, renewable energy and wastes, total electricity production	GHG emissions	-	Compared with SVM 85% data used for training and 15% data used for testing
20	[160]	MLP 4-20-1	AGRIS on-line Papers in Economics and Informatics	Apulia, Italia	CO <sub>2</sub> (t - 1), CO <sub>2</sub> (t - 2), CO <sub>2</sub> (t - 3), ma (CO <sub>2</sub> (t-3)), CO <sub>2</sub> (t - 2), CO <sub>2</sub> (t - 1))	CO <sub>2</sub> (t)	sigmoid (output layer)	Trained by LM algorithm Input data normalized to [0, 1]
21	[161]	MLP 5-40-30-1	Water	-	lat, lon, reservoir age, mean depth, surface area	CH <sub>4</sub>	tansig (hidden layer) purelin (output layer)	Trained by LM BP algorithm Input data normalized to [-1, 1]
22	[162]	MLP 36-36-1	Science of The Total Environment	Seoul, South Korea	Concentrations at 14:00, meteorological conditions at 14:00, variation velocity between 13:00 and 14:00, 08:00 and 14:00, 11:00 and 14:00, O <sub>3</sub> concentration	O <sub>3</sub> concentration at 15:00	sigmoid (output layer) purelin (output layer)	-

					s at 08:00, 11:00 and 13:00			
23	[163]	MLP 16-8-1	Transportation Research Part D: Transport and Environment	Guangzhou, China	Traffic volume, t (hour), t (day), T, P, W <sub>s</sub> , W <sub>d</sub> , G, rainfall, RH, concentration 1st hour before, 2nd, 3rd, distance to road center line, street direction, street aspect ratio	CO, NO <sub>2</sub> , PM <sub>10</sub> , O <sub>3</sub>	sigmoid (output layer)	Trained by BP algorithm Input data normalized to [0, 1] 495 groups used for training, 24 groups used for evaluation, and 42 groups used for testing
24	[164]	MLP 6-3-1	Applied Sciences	Malaysia	Car numbers, heavy vehicle numbers, S/M, T, W <sub>s</sub> , digital surface model (DSM)	Daily traffic CO emissions	tansig (hidden layer)	Correlation-based feature selection (CFS) model algorithm is adopted 70% data used for training and 30% data used for testing

Due to limitations on the length of the article, only 24 investigations have been selected as the most representative. However, other findings, such as those of [165–168], are also in the same direction. The main characteristics of the networks studied are detailed below.

- ANN type: as in all previous sections, the MLP has been the structure chosen by most researchers (21 out of 24 cases). Research has also been found that has made use of the GRNN [149] and Elman NN [146]. The use of GRNN is motivated by the fact that they only require a selection of parameters [169], do not need training, and work well with small data [170].
- Structure of the ANN: most of the studies analyzed use simple structures with a single hidden layer (21 out of 24 cases), with two hidden layers used in all other cases. The number of neurons in the hidden layer is of the order of 10.
- Amount of data: in most research, the volume of data is in the order of hundreds or thousands. Normally, a major part of the data is used for training, with the remainder being applied to testing. The percentage of research that makes use of data for validation is 35.3% (6 out of 17 cases).
- I/O configuration: the networks take different greenhouse gases such as CO<sub>2</sub>, CO, CH<sub>4</sub>, NO<sub>x</sub>, SO<sub>2</sub>, O<sub>3</sub>, PM<sub>10</sub>, and F-gases as output, while in most research, the inputs are macroeconomic or meteorological variables.
- Activation function: only 3 of the 24 investigations do not specify the activation function used. In the hidden layer, linear functions are used, with tansig and logsig being the most used, while in the output layer, the purelin and sigmoid types are adopted.

#### 4. Contest Analysis

In this section, the results obtained from the analysis of trends in the use of ANNs in renewable energies and for GHG prediction detailed in the previous sections were compared. As can be seen and already confirmed by Srisamranrungruang and K. Hiyama in

2022, artificial neural networks (ANN) are an essential element of deep learning in artificial intelligence (AI), reaching enormous relevance in applications such as the use of renewable energy.

In addition, Olanrewaju et al. concluded in 2022 that ANNs were very useful when modeling renewable energy systems, such as complex mapping of energy resources, and demonstrated that the errors that could be made with the use of ANNs were within the limits of acceptable tolerances.

4.1. Analysis of the Research Trend Based on the Year of Publication, Country, and Number of Publications by Type of Application

The review of the research articles revealed that the level of publications in relation to the three aspects analyzed was similar. Wind power and speed prediction generated 25 articles, very similar to the 24 articles for GHG prediction, followed by 20 articles on wave prediction and 17 on solar energy prediction. The first research article was published in 1996 and, except for 1997 and 2017, in every year until 2021, research was published on the topics analyzed.

The annual trend for each type of research is shown in Figure 6.

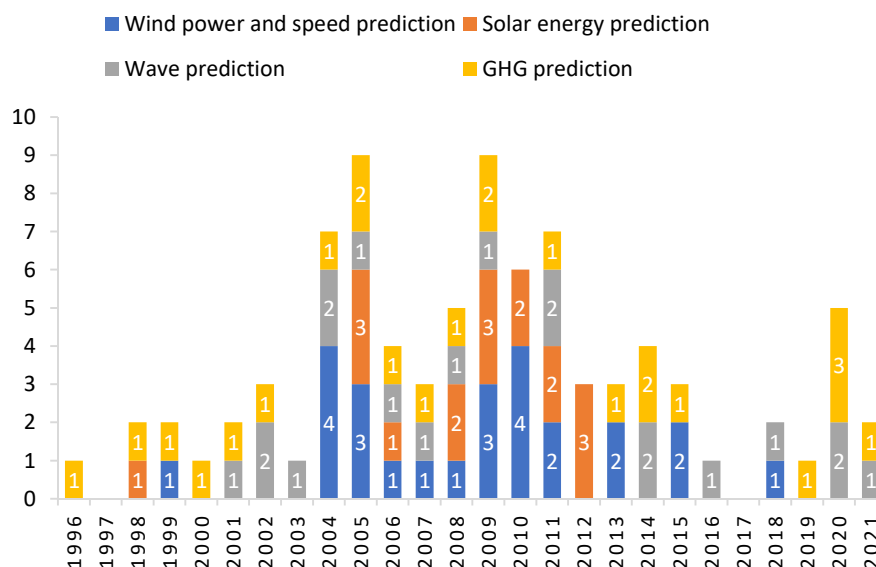


Figure 6. Number of annual publications for each type of research.

4.2. Countries with the Highest Number of Research

Research carried out by 30 countries has been published and interest in the subject extends to all continents. Figure 7 shows that the interest in the different research analyzed maintains a constant distribution. However, a special interest in wave prediction is observed in the USA as well as in India. This last country also stands out for the number of publications on GHG prediction. Turkey’s first place as the country with the highest number of publications on solar energy prediction is also particularly relevant.



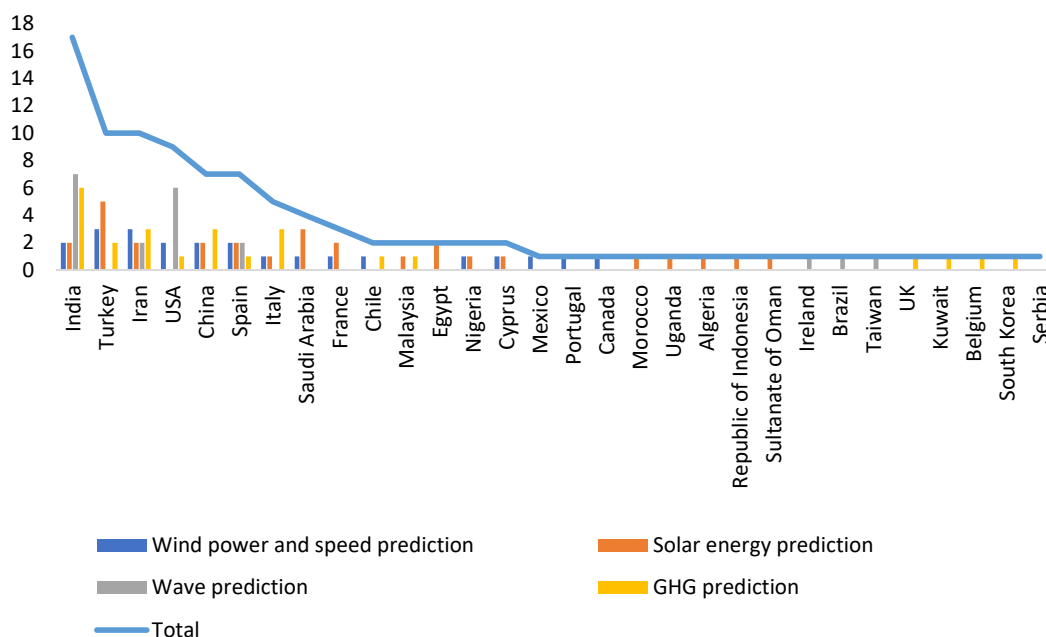


Figure 7. Number of research published by country.

4.3. Methodological Preferences in Research Carried out with ANNs and Types for the Different Applications

Figure 8 presents the different network structures used. Most of the investigations opted for MLP as the ANN type. The use of MLP is especially predominant in GHG prediction and solar energy prediction.

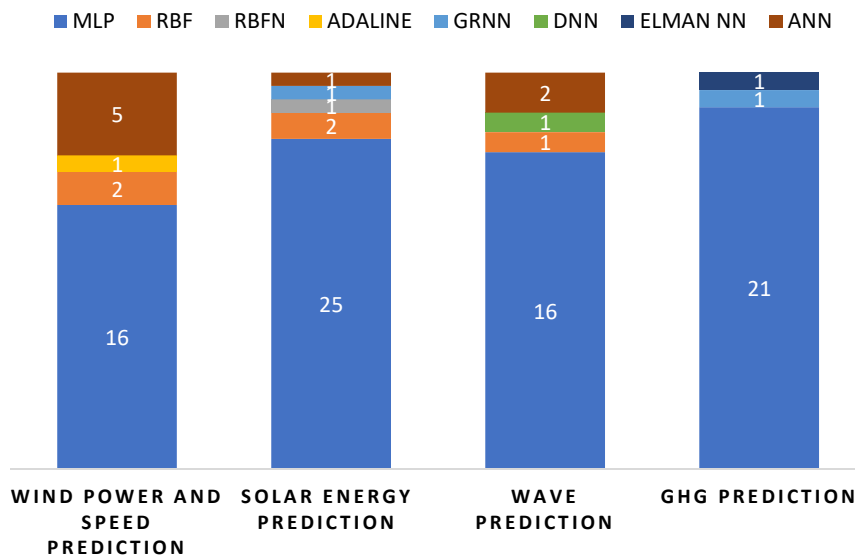


Figure 8. Network structures used with each research.

4.4. Trends in Publishing on Applications of Artificial Neural Networks to Energy Transition and Journals with Higher Productivity

The interest in the subject matter is evident from the large number of prestigious journals that have published research articles, as can be seen in Figures 9–11. Although some journals are repeated in the three investigations, each one of them presents a type of journal influenced by its area of research.

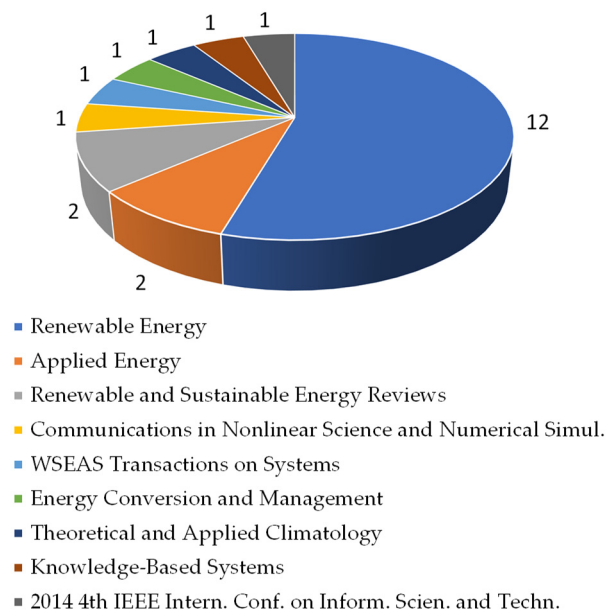


Figure 9. Journals with higher productivity in ANNs for wind power and speed prediction.

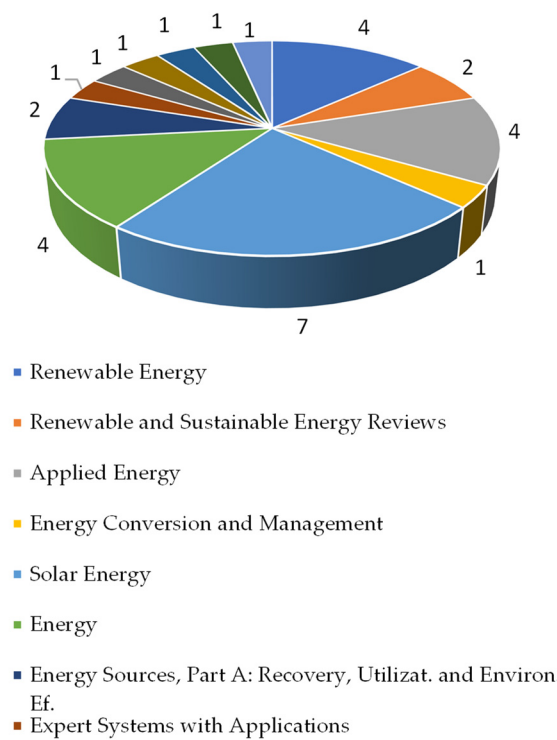


Figure 10. Journals with higher productivity in ANNs for solar energy prediction.

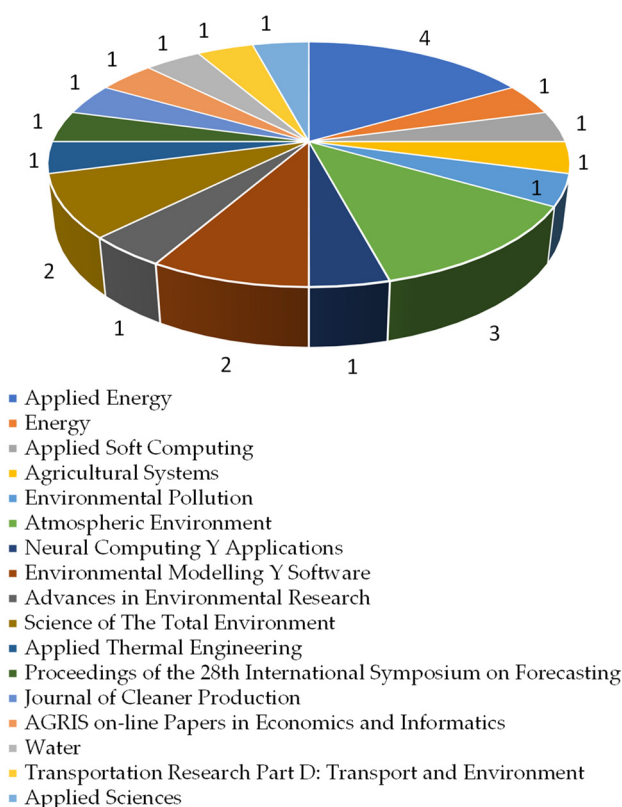


Figure 11. Journals with higher productivity in ANNs for GHD prediction.

#### 4.5. Most Used Activation Functions

Figure 12 shows the trend regarding the use of the 37 types of activation functions used in the different investigations. purelin (output layer) and tansig (hidden layer) turned out to be the most used for wind power and speed prediction. For wave prediction, purelin (output layer) and sigmoid (output layer) stood out, while for solar energy prediction, the most used were purelin (output layer), tansig (hidden layer), and logsig (hidden layer). For GHG prediction, the most used were purelin (output layer), tansig (hidden layer), and sigmoid (hidden layer).

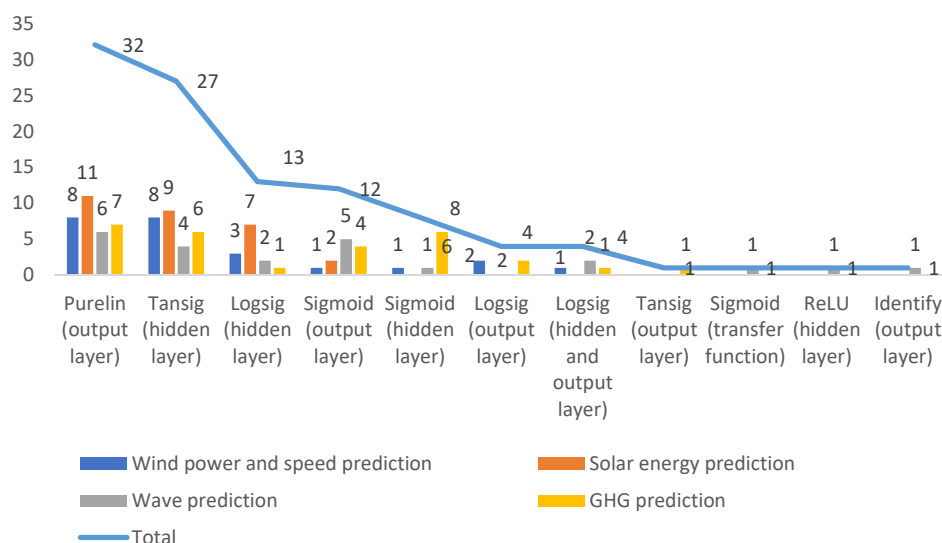


Figure 12. Trend in the use of activation functions.

## 5. Conclusions

The ANNs turned out to be a reliable and mature model for forecasting energy resources and the level of associated pollutant emissions.

The great interest in the subject has led to the publication of research in a wide variety of prestigious scientific journals. In particular, the level of productivity of two magazines stands out: *Renewable Energy* and *Applied Energy*, with 18% and 10%, respectively, of the total published. These two journals belong to the Elsevier publishing house. Their areas of knowledge are energy and fuel and green and sustainable science and technology and energy and fuel and chemical engineering, presenting JCR indexes and Q1 quartiles.

The descriptive analysis of the journal articles together with the analysis of their content allowed for the finding of similarities regarding the use of ANN type. Both in the applications of ANN to renewable energies and in the applications of ANNs for GHG prediction, the most used ANN type was the MLP, used in 80% of the research.

This article aims to provide a detailed description of the existing literature on the different applications of ANNs to the energy transition. It includes relevant aspects such as the use of renewable energies and the reduction in GHG. Additionally, the analysis of results will provide future research with data on current trends in the management of ANN and existing limitations.

Although the research results have been published throughout the world and in 30 different countries, 80% of the research is concentrated in India, Turkey, Iran, USA, China, Spain, Italy, and Saudi Arabia. Especially relevant is the contribution of India with almost 20% of the total.

The analyzed research began in 1996, focusing on GHG prediction and extended until 2022. The years with the highest number of publications were 2005 and 2009. In addition, the rate of publications remained constant over the years, with a significant resurgence of publications in 2020, confirming the interest in the topic. In this way, the use of ANNs presents a sufficient temporal development to demonstrate its usefulness and compete with the use of other algorithms. Some variables were difficult to model with ANN, for example, environmental variables due to the large number of associated uncertainties. However, the ANN turned out to be a valid prediction aid. Thus, ANNs occupy a central place in the transition due to their ability to learn and decide and are increasingly present in intelligent systems. As it has been shown, ANNs are very useful in the field of renewable energies for predicting wind speed, solar radiation, or wave height. This is of great importance for the design of efficient energy systems, capable of anticipating and adapting to future phenomena. Therefore, it is considered necessary that further research should reinforce efforts to develop networks capable of a wider range of predictions with a smaller number of variables.

Likewise, there is also abundant literature for predicting energy consumption in buildings and traffic as well as forecasting the pollutant emissions of a given activity. Although a large number of contributions have been found in the aforementioned sectors, it would be necessary to extend the use of ANNs to all sectors that make up a country's energy scenario, such as manufacturing, construction, agriculture, and mining, among others. This is really useful as it opens the way to the development of new applications capable of predicting the energy of a complete national energy system, thus making our energy systems more competitive, safe, and sustainable. As a result, world energy systems will be in a position to meet current global environmental commitments.

On the other hand, the type of architecture most chosen by the researchers was the multilayer perceptron, while the algorithms most used for training were backpropagation and Levenberg–Marquardt. The choice of MLP as the most used network is based on the fact that it is the most suitable ANN for classification and prediction. Moreover, the most used activation functions were purelin (output layer) and tansig (hidden layer). They stood out in the four investigations carried out. In addition, logsig (hidden layer) was also widely used in the case of solar energy prediction, as was sigmoid (output layer) for wave

prediction and sigmoid (hidden layer) for GHG prediction. It is also noteworthy that research in which the greatest variety of activation functions was observed was the wave prediction with nine different activation functions, compared to the solar energy prediction with only four types.

The results and analysis performed with ANNs in this study can serve as a guide for the parties involved in the energy transition, in decision making, and in planning concrete actions to achieve the goals of increasing the contribution of renewable energy sources to the energy system, reducing GHG, and improving energy efficiency. Several methods can be used to communicate ANN results and recommendations to stakeholders. These can range from detailed technical reports for technical stakeholders to user manuals or graphs and diagrams for less technical or business-oriented end users. Data and information can also be reflected in technical equipment, through control panels of generation and distribution units, feedback loops, or other types of technical and informational channels.

As it has been seen, the largest number of contributions of ANR to the energy transition are focused on both renewable energy and greenhouse gas emissions. While these are the pillars of EU and international energy policy, it would be desirable to further develop new applications with a view to achieving fully efficient, secure, and sustainable energy systems.

Future research work could analyze research trends with ANNs in other aspects related to the energy transition, such as the generation and use of energy-recoverable biomass. In addition, the study of these techniques in the use of both residual biomass and specific crops could be useful to properly value the use of this resource and avoid increases in food prices. Another line of work could be the analysis of the application of the ANN in new sustainable mobility. Thus, the efficient control of freight traffic and private travel would be of great importance in reducing the level of polluting emissions associated with transport. Other future lines of research could be to try to find sufficient data to measure the diagnostic performance of ANNs using the receiver operating characteristic (ROC) method.

**Author Contributions:** Conceptualization, Í.M.I.-S.C. and A.M.-F.; methodology, Í.M.I.-S.C., A.J.G.-T., J.C.R.-F. and A.M.-F.; software, Í.M.I.-S.C.; validation, A.J.G.-T.; formal analysis, Í.M.I.-S.C., A.J.G.-T., J.C.R.-F. and A.M.-F.; investigation, Í.M.I.-S.C., A.J.G.-T., J.C.R.-F. and A.M.-F.; resources, Í.M.I.-S.C.; data curation, Í.M.I.-S.C., A.J.G.-T., J.C.R.-F. and A.M.-F.; writing—original draft preparation, Í.M.I.-S.C., A.J.G.-T., J.C.R.-F. and A.M.-F.; writing—review and editing, A.J.G.-T. and J.C.R.-F.; supervision, A.J.G.-T.; project administration, A.J.G.-T. and J.C.R.-F. All authors have read and agreed to the published version of the manuscript.

**Funding:** This research did not receive any specific grant from funding agencies in the public, commercial, or not-for-profit sectors.

**Institutional Review Board Statement:** Not applicable.

**Informed Consent Statement:** Not applicable.

**Data Availability Statement:** Not applicable.

**Conflicts of Interest:** The authors declare no conflicts of interests.

## Abbreviations

ANNs	artificial neural networks
MDPI	Multidisciplinary Digital Publishing Institute
AI	artificial intelligence
GA	genetic algorithms
FL	fuzzy logic
BP	backpropagation
UN	United Nations
MLP	multilayer perceptron
$W_s$	wind speed
Lon	longitude

Lat	latitude
A	altitude
RBF	radial basis function
$W_d$	wind direction
$W_p$	wind power
M	month
RP	resilient propagation
LM	Levenberg–Marquardt
ICA	imperialist competitive algorithm
PSO	particle swarm optimization
BR	Bayesian regularized
T	temperature
$T_{AVG}$	average temperature
$T_{max}$	maximum temperature
$T_{min}$	minimum temperature
$P_{air}$	air pressure
G	solar irradiance
$T_{air}$	air temperature
SCG	scaled conjugate gradient
IEEE	International Conference on Information Science and Technology
P	pressure
I/O	input/output
GRNN	general regression neural network
$P_w$	power
S	sunshine duration
Y	nebulosity
DGP	differential pressure
$K_T$	clearness index
t	hour or day
$G_D$	daily global solar radiation
$k_t$	hourly clearness index
$S_{0d}$	theoretical sunshine duration
TCC	total cloud cover
$K_D$	diffuse fraction
$\varepsilon_4$	surface emissivity
$\varepsilon_5$	surface emissivity
$R_a$	terrestrial radiation
L	location
H	height
DNN	deep neural network
$H_o$	deep-water wave height
$T_e$	wave energy period
$H_b$	breaking wave height
$d_b$	water depth at the time of breaking
$T_p$	H and zero-up-crossing peak wave period
$F_e$	energy flux
W	weather station index
U	wind shear velocity
ANFIS	adaptive neuro-fuzzy inference system
$H_{1/3}$	significant wave height
$H_{1/10}$	highest one-tenth wave height
$H_{max}$	highest wave height
$H_{mean}$	mean wave height
CGB	conjugate gradient Powell–Beale
BFG	Broyden–Fletcher–Goldfarb
$T_p$	wave direction
GHG	greenhouse gases

GAINS	greenhouse gas and air pollution interactions and synergies
N	nitrogen
P <sub>2</sub> O <sub>5</sub>	phosphate
K <sub>2</sub> O	potassium
FYM	farmyard manure
O <sub>3</sub>	ozone
CO <sub>2</sub>	carbon dioxide
NO	nitric oxide
NO <sub>2</sub>	nitrogen dioxide
NO <sub>x</sub>	oxide of nitrogen
LOW	low cloud amount
BASE	base of lowest cloud
VIS	visibility
CO	carbon monoxide
CH <sub>4</sub>	methane
GDP	gross domestic product
GIEC	gross inland energy consumption
BLH	boundary layer height
PrIT	pre-injection timing
MIT	main injection timing
PIT	post-injection timing
UBHC	unburned hydrocarbon
TP	throttle position
LHV	lower heating value
BSFC	brake-specific fuel consumption
BTh	brake thermal efficiency
$\eta_v$	volumetric efficiency
EGT	exhaust gas temperature
CFS	correlation-based feature selection
AI	artificial intelligence

## References

1. Youssef, A.; El-Telbany, M.; Zekry, A. The role of artificial intelligence in photo-voltaic systems design and control: A review. *Renew. Sustain. Energy Rev.* **2017**, *78*, 72–79.
2. Jani, D.; Mishra, M.; Sahoo, P. Application of artificial neural network for predicting performance of solid desiccant cooling systems—A review. *Renew. Sustain. Energy Rev.* **2017**, *80*, 352–366.
3. McCulloch, W.S.; Pitts, W. A logical calculus of the ideas immanent in nervous activity. *Bull. Math. Biophys.* **1943**, *5*, 115–133.
4. Hebb, D.O. The first stage of perception: Growth of the assembly. *Organ. Behav.* **1949**, *4*, 78–60.
5. Miller, D.D.; Brown, E.W. Artificial intelligence in medical practice: The question to the answer? *Am. J. Med.* **2018**, *131*, 129–133.
6. Widrow, B.; Hoff, M.E. Adaptive switching circuits. In *IRE WESCON Convention Record*; Institute of Radio Engineers: New York, NY, USA, 1960; pp. 96–104.
7. Widrow, B. Ancient History. In *Cybernetics 2.0: A General Theory of Adaptivity and Homeostasis in the Brain and in the Body*; Springer International Publishing: Berlin/Heidelberg, Germany, 2022.
8. Minsky, M.; Papert, S. *Perceptrons. An Introduction to Computational Geometry*; The MIT Press Ltd.: Cambridge, MA, USA, 1969.
9. Olazaran, M. A sociological history of the neural network controversy. *Adv. Comput.* **1993**, *37*, 335–425.
10. Werbos, P. Beyond Regression: New Tools for Prediction and Analysts in the Behavioral Sciences. Ph.D. Thesis, Harvard University, Cambridge, MA, USA, 1974.
11. Werbos, P.J. Generalization of backpropagation with application to a recurrent gas market model. *Neural Netw.* **1988**, *1*, 339–356.
12. Gholamalinezhad, H.; Khosravi, H. Pooling methods in deep neural networks, a review. *arXiv* **2020**, arXiv:2009.07485.
13. Zhu, X.; Goldberg, A.B. *Introduction to Semi-Supervised Learning*; Springer Nature: Berlin/Heidelberg, Germany, 2022.
14. Matsuo, Y.; LeCun, Y.; Sahani, M.; Precup, D.; Silver, D.; Sugiyama, M.; Uchibe, E.; Morimoto, J. Deep learning, reinforcement learning, and world models. *Neural Netw.* **2022**, *152*, 267–275.
15. Pérez-Suárez, A.; Martínez-Trinidad, J.F.; Carrasco-Ochoa, J.A. A review of conceptual clustering algorithms. *Artif. Intell. Rev.* **2019**, *52*, 1267–1296.
16. Dang, W.; Guo, J.; Liu, M.; Liu, S.; Yang, B.; Yin, L.; Zheng, W. A Semi-Supervised Extreme Learning Machine Algorithm Based on the New Weighted Kernel for Machine Smell. *Appl. Sci.* **2022**, *12*, 9213.

17. Nguyen, V.L.; Shaker, M.H.; Hüllermeier, E. How to measure uncertainty in uncertainty sampling for active learning. *Mach. Learn.* **2022**, *111*, 89–122.
18. Peirelinck, T.; Kazmi, H.; Mbuwir, B.V.; Hermans, C.; Spiessens, F.; Suykens, J.; Deconinck, G. Transfer learning in demand response: A review of algorithms for data-efficient modelling and control. *Energy AI* **2022**, *7*, 100126.
19. Wang, J.; Lu, S.; Wang, S.H.; Zhang, Y.D. A review on extreme learning machine. *Multimed. Tools Appl.* **2022**, *81*, 41611–41660.
20. Whang, S.E.; Roh, Y.; Song, H.; Lee, J.G. Data collection and quality challenges in deep learning: A data-centric AI perspective. *VLDB J.* **2023**, *32*, 791–813.
21. Sze, V.; Chen, Y.H.; Yang, T.J.; Emer, J.S. Efficient processing of deep neural networks: A tutorial and survey. *Proc. IEEE* **2017**, *105*, 2295–2329.
22. Roh, Y.; Heo, G.; Whang, S.E. A survey on data collection for machine learning: A big data—AI integration perspective. *IEEE Trans. Knowl. Data Eng.* **2019**, *33*, 1328–1347.
23. Su, X.; Zhao, Y.; Bethard, S. A comparison of strategies for source-free domain adaptation. In Proceedings of the 60th Annual Meeting of the Association for Computational Linguistics, Dublin, Ireland, 22–27 May 2022; pp. 8352–8367.
24. Abiodun, O.; Jantan, A.; Omolara, A.; Dada, K.; Mohamed, N.; Arshad, H. State-of-the-art in artificial neural network applications: A survey. *Heliyon* **2018**, *4*, e00938.
25. Costa, Á.; Markellos, R.N. Evaluating public transport efficiency with neural network models. *Transp. Res. Part C Emerg. Technol.* **1997**, *5*, 301–312.
26. Abdou, M.A. Literature review: Efficient deep neural networks techniques for medical image analysis. *Neural Comput. Appl.* **2022**, *34*, 5791–5812.
27. Le, T.H. Applying Artificial Neural Networks for Face Recognition. *Adv. Artif. Neural Syst.* **2011**, *2011*, 673016.
28. Santín, D.; Delgado, F.J.; Valiño, A. The measurement of technical efficiency: A neural network approach. *Appl. Econ.* **2004**, *36*, 627–635.
29. Labidi, J.; Pelach, M.A.; Turon, X.; Mutje, P. Predicting flotation efficiency using neural networks. *Chem. Eng. Process. Process Intensif.* **2007**, *46*, 314–322.
30. Li, B.; Delpha, C.; Diallo, D.; Migan-Dubois, A. Application of Artificial Neural Networks to photovoltaic fault detection and diagnosis: A review. *Renew. Sustain. Energy Rev.* **2021**, *138*, 110512.
31. Abarghouei, A.A.; Ghanizadeh, A.; Shamsuddin, S.M. Advances of soft computing methods in edge detection. *Int. J. Adv. Soft Comput. Its Appl.* **2009**, *1*, 162–203.
32. Hamad, K.; Khalil, M.A.; Shanableh, A. Modeling roadway traffic noise in a hot climate using artificial neural networks. *Transp. Res. Part D Transp. Environ.* **2017**, *53*, 161–177.
33. Karabacak, K.; Cetin, N. Artificial neural networks for controlling wind–PV power systems: A review. *Renew. Sustain. Energy Rev.* **2014**, *29*, 804–827.
34. Rojas, R. *Neural Networks: A Systematic Introduction*; Springer Science Y Business Media: Berlin/Heidelberg, Germany, 2013.
35. Mohanraj, M.; Jayaraj, S.; Muraleedharan, C. Applications of artificial neural networks for refrigeration, air-conditioning and heat pump systems—A review. *Renew. Sustain. Energy Rev.* **2012**, *16*, 1340–1358.
36. Yin, C.; Rosendahl, L.; Luo, Z. Methods to improve prediction performance of ANN models. *Simul. Model. Pr. Theory* **2003**, *11*, 211–222.
37. Yang, K. Artificial Neural Networks (ANNs): A New Paradigm for Thermal Science and Engineering. *J. Heat Transf.* **2008**, *130*, 093001.
38. Poznyak, T.I.; Oria, I.C.; Poznyak, A.S. Chapter 3—Background on dynamic neural networks. *Ozonation Biodegrad. Environ. Eng.* **2019**, 57–74.
39. Rosenblatt, F. The perceptron: A probabilistic model for information storage and organization in the brain. *Psychol. Rev.* **1958**, *65*, 386–408.
40. Poznyak, A.S.; Sanchez, E.N.; Yu, W. *Differential Neural Networks for Robust Nonlinear Control: Identification, State Estimation and Trajectory Tracking*; World Scientific: Singapore, 2001.
41. Hecht-Nielsen, R. Theory of the backpropagation neural network. In *Neural Networks for Perception*; Academic Press: Cambridge, MA, USA, 1992; pp. 65–93.
42. Elsheikh, A.H.; Sharshir, S.W.; Abd Elaziz, M.; Kabeel, A.E.; Guilan, W.; Haiou, Z. Modeling of solar energy systems using artificial neural network: A comprehensive review. *Sol. Energy* **2019**, *180*, 622–639.
43. Wang, S.; Zhou, R.; Zhao, L. Forecasting Beijing transportation hub areas’s pedestrian flow using modular neural network. *Discret. Dyn. Nat. Soc.* **2015**, *2015*, 749181.
44. Bhaskar, K.; Singh, S.N. AWNN-assisted wind power forecasting using feed-forward neural network. *IEEE Trans. Sustain. Energy* **2012**, *3*, 306–315.
45. Tran, D.; Tan, Y.K. Sensorless illumination control of a networked LED-lighting system using feedforward neural network. *IEEE Trans. Ind. Electron.* **2013**, *61*, 2113–2121.
46. Suykens, J.; Vandewalle, J.; Moor, B. *Artificial Neural Networks for Modelling and Control of Non-Linear Systems*; Springer Science Y Business Media: Berlin/Heidelberg, Germany, 1995.
47. Karthigayani, P.; Sridhar, S. Decision tree based occlusion detection in face recognition and estimation of human age using back propagation neural network. *J. Comput. Sci.* **2014**, *10*, 115–127.



48. Buzhinsky, I.; Nerinovsky, A.; Tripakis, S. Metrics and methods for robustness evaluation of neural networks with generative models. *Mach. Learn.* **2021**, *112*, 3977–4012.
49. Levy, N.; Katz, G. Roma: A method for neural network robustness measurement and assessment. In Proceedings of the International Conference on Neural Information Processing, Virtual, 22–26 November 2022; pp. 92–105.
50. Kamel, A.R.; Alqarni, A.A.; Ahmed, M.A. On the Performance Robustness of Artificial Neural Network Approaches and Gumbel Extreme Value Distribution for Prediction of Wind Speed. *Int. J. Sci. Res. Math. Stat. Sci.* **2022**, *9*, 5–22.
51. Savva, A.G.; Theocharides, T.; Nicopoulos, C. Robustness of Artificial Neural Networks Based on Weight Alterations Used for Prediction Purposes. *Algorithms* **2023**, *16*, 322.
52. Nishant, R.; Kennedy, M.; Corbett, J. Artificial intelligence for sustainability: Challenges, opportunities, and a research agenda. *Int. J. Inf. Manag.* **2020**, *53*, 102104.
53. Danish, M.S.S.; Senjyu, T. Shaping the future of sustainable energy through AI-enabled circular economy policies. *Circ. Econ.* **2023**, *2*, 100040.
54. Camilleri, M.A. Artificial intelligence governance: Ethical considerations and implications for social responsibility. *Expert Syst.* **2023**, e13406.
55. Roberts, H.; Zhang, J.; Bariach, B.; Cowls, J.; Gilbert, B.; Juneja, P.; Tsamados, A.; Ziosi, M.; Taddeo, M.; Floridi, L. Artificial intelligence in support of the circular economy: Ethical considerations and a path forward. *AI Soc.* **2022**, 1–14.
56. Crane, A.; McWilliams, A.; Matten, D.; Moon, J.; Siegel, D.S. *The Oxford Handbook of Corporate Social Responsibility*; OUP Oxford: Oxford, UK, 2008.
57. Tai, M.-T. The impact of artificial intelligence on human society and bioethics. *Tzu Chi Med. J.* **2020**, *32*, 339–343.
58. Wilson, H.J.; Daugherty, P.R. Collaborative intelligence: Humans and AI are joining forces. *Harv. Bus. Rev.* **2018**, *96*, 114–123.
59. Eurostat. Eurostat Statics Explained. 2019. Available online: [https://ec.europa.eu/eurostat/statistics-explained/index.php?title=Renewable\\_energy\\_statistics#Wind\\_and\\_water\\_provide\\_most\\_renewable\\_electricity.3B\\_solar\\_is\\_the\\_fastest-growing\\_energy\\_source](https://ec.europa.eu/eurostat/statistics-explained/index.php?title=Renewable_energy_statistics#Wind_and_water_provide_most_renewable_electricity.3B_solar_is_the_fastest-growing_energy_source) (accessed on 30 December 2023).
60. Noorollahi, Y.; Jokar, M.A.; Kalhor, A. Using artificial neural networks for temporal and spatial wind speed forecasting in Iran. *Energy Convers. Manag.* **2016**, *115*, 17–25.
61. Mabel, M.C.; Fernandez, E. Analysis of wind power generation and prediction using ANN: A case study. *Renew. Energy* **2008**, *33*, 986–992.
62. Çam, E.; Arcaklıoğlu, E.; Çavuşoğlu, A.; Akbıyık, B. A classification mechanism for determining average wind speed and power in several regions of Turkey using artificial neural networks. *Renew. Energy* **2005**, *30*, 227–239.
63. Bilgili, M.; Sahin, B.; Yasar, A. Application of artificial neural networks for the wind speed prediction of target using reference stations data. *Renew. Energy* **2007**, *32*, 2350–2360.
64. Assareh, E.; Biglari, M. A novel approach to capture the maximum power from variable speed wind turbines using PI controller, RBF neural network and GSA evolutionary algorithm. *Renew. Sustain. Energy Rev.* **2015**, *51*, 1023–1037.
65. Mohandes, M.; Halawani, T.; Rehman, S.; Hussain, A.A. Support vector machines for wind speed prediction. *Renew. Energy* **2004**, *29*, 939–947.
66. Bigdeli, N.; Afshar, K.; Gazafroudi, A.S.; Ramandi, M.Y. A comparative study of optimal hybrid methods for wind power prediction in wind farm of Alberta, Canada. *Renew. Sustain. Energy Rev.* **2013**, *27*, 20–29.
67. Manobel, B.; Sehnke, F.; Lazzús, J.A.; Salfate, I.; Felder, M.; Montecinos, S. Wind turbine power curve modeling based on Gaussian Processes and Artificial Neural Networks. *Renew. Energy* **2018**, *125*, 1015–1020.
68. Li, G.; Shi, J. On comparing three artificial neural networks for wind speed forecasting. *Appl. Energy* **2010**, *87*, 2313–2320.
69. Blonbou, R. Very short-term wind power forecasting with neural networks and adaptive Bayesian learning. *Renew. Energy* **2011**, *36*, 1118–1124.
70. Liu, H.; Tian, H.-Q.; Chen, C.; Li, Y.-F. A hybrid statistical method to predict wind speed and wind power. *Renew. Energy* **2010**, *35*, 1857–1861.
71. Salcedo-Sanz, S.; Pérez-Bellido, Á.M.; Ortiz-García, E.G.; Portilla-Figueras, A.; Prieto, L.; Paredes, D. Hybridizing the fifth generation mesoscale model with artificial neural networks for short-term wind speed prediction. *Renew. Energy* **2009**, *34*, 1451–1457.
72. Cadenas, E.; Rivera, W. Short term wind speed forecasting in La Venta, Oaxaca, México, using artificial neural networks. *Renew. Energy* **2009**, *34*, 274–278.
73. Flores, P.; Tapia, A.; Tapia, G. Application of a control algorithm for wind speed prediction and active power generation. *Renew. Energy* **2005**, *30*, 523–536.
74. Monfared, M.; Rastegar, H.; Kojabadi, H.M. A new strategy for wind speed forecasting using artificial intelligent methods. *Renew. Energy* **2009**, *34*, 845–848.
75. Grassi, G.; Vecchio, P. Wind energy prediction using a two-hidden layer neural network. *Commun. Nonlinear Sci. Numer. Simul.* **2010**, *15*, 2262–2266.
76. Ramasamy, P.; Chandel, S.; Yadav, A.K. Wind speed prediction in the mountainous region of India using an artificial neural network model. *Renew. Energy* **2015**, *80*, 338–347.
77. Fadare, D. The application of artificial neural networks to mapping of wind speed profile for energy application in Nigeria. *Appl. Energy* **2010**, *87*, 934–942.

78. Fonte, P.M.; Silva, G.X.; Quadrado, J.C. Wind speed prediction using artificial neural networks. *WSEAS Trans. Syst.* **2005**, *4*, 379–384.
79. Kalogirou, S.; Neocleous, C.; Pashiardis, S.; Schizas, C. Wind speed prediction using artificial neural networks. In Proceedings of the European Symposium on Intelligent Techniques, Crete, Greece, 3–4 June 1999.
80. Öztopal, A. Artificial neural network approach to spatial estimation of wind velocity data. *Energy Convers. Manag.* **2006**, *47*, 395–406.
81. Ghorbani, M.A.; Khatibi, R.; Hosseini, B.; Bilgili, M. Relative importance of parameters affecting wind speed prediction using artificial neural networks. *Theor. Appl. Clim.* **2013**, *114*, 107–114.
82. Guo, Z.-H.; Wu, J.; Lu, H.-Y.; Wang, J.-Z. A case study on a hybrid wind speed forecasting method using BP neural network. *Knowl.-Based Syst.* **2011**, *24*, 1048–1056.
83. Lodge, A.; Yu, X. Short term wind speed prediction using artificial neural networks. In Proceedings of the 4th IEEE International Conference on Information Science and Technology, Shenzhen, China, 26–28 April 2014.
84. Le, X.C.; Duong, M.Q.; Le, K.H. Review of the Modern Maximum Power Tracking Algorithms for Permanent Magnet Synchronous Generator of Wind Power Conversion Systems. *Energies* **2022**, *16*, 402.
85. Mellit, A.; Kalogirou, S.; Hontoria, L.; Shaari, S. Artificial intelligence techniques for sizing photovoltaic systems: A review. *Renew. Sustain. Energy Rev.* **2009**, *13*, 406–419.
86. Mellit, A.; Kalogirou, S.A. Artificial intelligence techniques for photovoltaic applications: A review. *Prog. Energy Combust. Sci.* **2008**, *34*, 574–632.
87. Ghritlahre, H.K.; Prasad, R.K. Application of ANN technique to predict the performance of solar collector systems—A review. *Renew. Sustain. Energy Rev.* **2018**, *84*, 75–88.
88. Yadav, A.K.; Chandel, S. Solar radiation prediction using Artificial Neural Network techniques: A review. *Renew. Sustain. Energy Rev.* **2014**, *33*, 772–781.
89. Chen, C.; Duan, S.; Cai, T.; Liu, B. Online 24-h solar power forecasting based on weather type classification using artificial neural network. *Sol. Energy* **2011**, *85*, 2856–2870.
90. Almonacid, F.; Rus, C.; Pérez, P.J.; Hontoria, L. Estimation of the energy of a PV generator using artificial neural network. *Renew. Energy* **2009**, *34*, 2743–2750.
91. Voyant, C.; Muselli, M.; Paoli, C.; Nivet, M.-L. Optimization of an artificial neural network dedicated to the multivariate forecasting of daily global radiation. *Energy* **2011**, *36*, 348–359.
92. Paoli, C.; Voyant, C.; Muselli, M.; Nivet, M.-L. Forecasting of preprocessed daily solar radiation time series using neural networks. *Sol. Energy* **2010**, *84*, 2146–2160.
93. Mellit, A.; Pavan, A.M. A 24-h forecast of solar irradiance using artificial neural network: Application for performance prediction of a grid-connected PV plant at Trieste, Italy. *Sol. Energy* **2010**, *84*, 807–821.
94. Benganem, M.; Mellit, A. Radial Basis Function Network-based prediction of global solar radiation data: Application for sizing of a stand-alone photovoltaic system at Al-Madinah, Saudi Arabia. *Energy* **2010**, *35*, 3751–3762.
95. Sözen, A.; Arcaklioğlu, E.; Özalp, M.; Kanit, E. Use of artificial neural networks for mapping of solar potential in Turkey. *Appl. Energy* **2004**, *77*, 273–286.
96. Ouammi, A.; Zejli, D.; Dagdougui, H.; Benchrifa, R. Artificial neural network analysis of Moroccan solar potential. *Renew. Sustain. Energy Rev.* **2012**, *16*, 4876–4889.
97. Rehman, S.; Mohandes, M. Estimation of Diffuse Fraction of Global Solar Radiation Using Artificial Neural Networks. *Energy Sources Part A Recovery Util. Environ. Eff.* **2009**, *31*, 974–984.
98. Koca, A.; Oztop, H.F.; Varol, Y.; Koca, G.O. Estimation of solar radiation using artificial neural networks with different input parameters for Mediterranean region of Anatolia in Turkey. *Expert Syst. Appl.* **2011**, *38*, 8756–8762.
99. Fadare, D. Modelling of solar energy potential in Nigeria using an artificial neural network model. *Appl. Energy* **2009**, *86*, 1410–1422.
100. Khatib, T.; Mohamed, A.; Sopian, K.; Mahmoud, M. Solar Energy Prediction for Malaysia Using Artificial Neural Networks. *Int. J. Photoenergy* **2012**, *2012*, 419504.
101. Yadav, A.K.; Chandel, S.S. Artificial Neural Network based prediction of solar radiation for Indian stations. *Int. J. Comput. Appl.* **2012**, *50*, 1–4. <https://doi.org/10.5120/7796-0907>.
102. Elminir, H.K.; Azzam, Y.A.; Younes, F.I. Prediction of hourly and daily diffuse fraction using neural network, as compared to linear regression models. *Energy* **2007**, *32*, 1513–1523.
103. Hontoria, L.; Aguilera, J.; Zufiria, P. An application of the multilayer perceptron: Solar radiation maps in Spain. *Sol. Energy* **2005**, *79*, 523–530.
104. Elminir, H.K.; Areed, F.F.; Elsayed, T.S. Estimation of solar radiation components incident on Helwan site using neural networks. *Sol. Energy* **2005**, *79*, 270–279.
105. Tymvios, F.S.; Jacovides, C.P.; Michaelides, S.C.; Scouteli, C. Comparative study of Ångström's and artificial neural networks' methodologies in estimating global solar radiation. *Sol. Energy* **2005**, *78*, 752–762.
106. Alam, S.; Kaushik, S.C.; Garg, S.N. Computation of bean solar radiation at normal incidence using artificial neural network. *Renew. Energy* **2006**, *31*, 1483–1491.
107. Jiang, Y. Prediction of monthly mean daily diffuse solar radiation using artificial neural networks and comparison with other empirical models. *Energy Policy* **2008**, *36*, 3833–3837.

108. Mubiru, J.; Banda, E. Estimation of monthly average daily global solar irradiation using artificial neural networks. *Sol. Energy* **2008**, *82*, 181–187.
109. Şenkal, O.; Kuleli, T. Estimation of solar radiation over Turkey using artificial neural network and satellite data. *Appl. Energy* **2009**, *86*, 1222–1228.
110. Şenkal, O. Modeling of solar radiation using remote sensing and artificial neural network in Turkey. *Energy* **2010**, *35*, 4795–4801.
111. Azadeh, A.; Maghsoudi, A.; Sohrabkhani, S. An integrated artificial neural networks approach for predicting global radiation. *Energy Convers. Manag.* **2009**, *50*, 1497–1505.
112. Sözen, A.; Arcaklioğlu, E. Solar potential in Turkey. *Appl. Energy* **2005**, *80*, 35–45.
113. Rahimikhoob, A. Estimating global solar radiation using artificial neural network and air temperature data in a semi-arid environment. *Renew. Energy* **2010**, *35*, 2131–2135.
114. Hasni, A.; Sehli, A.; Draoui, B.; Bassou, A.; Amieur, B. Estimating Global Solar Radiation Using Artificial Neural Network and Climate Data in the South-western Region of Algeria. *Energy Procedia* **2012**, *18*, 531–537.
115. Rumbayan, M.; Abudureyimu, A.; Nagasaka, K. Mapping of solar energy potential in Indonesia using artificial neural network and geographical information system. *Renew. Sustain. Energy Rev.* **2012**, *16*, 1437–1449.
116. Rehman, S.; Mohandes, M. Splitting Global Solar Radiation into Diffuse and Direct Normal Fractions Using Artificial Neural Networks. *Energy Sources Part A Recover. Util. Environ. Eff.* **2012**, *34*, 1326–1336.
117. Al-Alawi, S.M.; Al-Hinai, H.A. An ANN-based approach for predicting global radiation in locations with no direct measurement instrumentation. *Renew. Energy* **1998**, *14*, 199–204.
118. Makarynsky, O.; Pires-Silva, A.; Makarynska, D.; Ventura-Soares, C. Artificial neural networks in wave predictions at the west coast of Portugal. *Comput. Geosci.* **2005**, *31*, 415–424.
119. Londhe, S.N.; Panchang, V. One-Day Wave Forecasts Based on Artificial Neural Networks. *J. Atmospheric Ocean. Technol.* **2006**, *23*, 1593–1603.
120. Deo, M.; Jagdale, S. Prediction of breaking waves with neural networks. *Ocean Eng.* **2003**, *30*, 1163–1178.
121. Makarynsky, O. Improving wave predictions with artificial neural networks. *Ocean Eng.* **2004**, *31*, 709–724.
122. Hadadpour, S.; Etemad-Shahidi, A.; Kamranzad, B. Wave energy forecasting using artificial neural networks in the Caspian Sea. *Proceeding Inst. Civ. Eng.-Marit. Eng.* **2014**, *167*, 42–52.
123. Deo, M.C.; Jha, A.; Chaphekar, A.S.; Ravikant, K. Neural networks for wave forecasting. *Ocean Eng.* **2001**, *28*, 889–898.
124. Bento, P.; Pombo, J.; Mendes, R.; Calado, M.; Mariano, S. Ocean wave energy forecasting using optimised deep learning neural networks. *Ocean Eng.* **2021**, *219*, 108372.
125. Feng, X.; Ma, G.; Su, S.-F.; Huang, C.; Boswell, M.K.; Xue, P. A multi-layer perceptron approach for accelerated wave forecasting in Lake Michigan. *Ocean Eng.* **2020**, *211*, 107526.
126. Agrawal, J.; Deo, M. Wave parameter estimation using neural networks. *Mar. Struct.* **2004**, *17*, 536–550.
127. Kamranzad, B.; Etemad-Shahidi, A.; Kazeminezhad, M.H. Wave height forecasting in Dayyer, the Persian Gulf. *Ocean Eng.* **2011**, *38*, 248–255.
128. Castro, A.; Carballo, R.; Iglesias, G.; Rabuñal, J.R. Performance of artificial neural networks in nearshore wave power prediction. *Appl. Soft Comput.* **2014**, *23*, 194–201.
129. Malekmohamadi, I.; Bazargan-Lari, M.R.; Kerachian, R.; Nikoo, M.R.; Fallahnia, M. Evaluating the efficacy of SVMs, BNs, ANNs and ANFIS in wave height prediction. *Ocean Eng.* **2011**, *38*, 487–497.
130. Sánchez, A.S.; Rodrigues, D.A.; Fontes, R.M.; Martins, M.F.; de Araújo Kalid, R.; Torres, E.A. Wave resource characterization through in-situ measurement followed by artificial neural networks' modeling. *Renew. Energy* **2018**, *115*, 1055–1066.
131. Avila, D.; Marichal, G.N.; Padrón, I.; Quiza, R.; Hernández, . Forecasting of wave energy in Canary Islands based on Artificial Intelligence. *Appl. Ocean Res.* **2020**, *101*, 102189.
132. Jain, P.; Deo, M. Real-time wave forecasts off the western Indian coast. *Appl. Ocean Res.* **2007**, *29*, 72–79.
133. Kalra, R.; Deo, M.; Kumar, R.; Agarwal, V.K. RBF network for spatial mapping of wave heights. *Mar. Struct.* **2005**, *18*, 289–30.
134. Tsai, C.P.; Lin, C.; Shen, J.N. Neural network for wave forecasting among multi-stations. *Ocean. Eng.* **2002**, *29*, 1683–1695.
135. Agrawal, J.; Deo, M. On-line wave prediction. *Mar. Struct.* **2002**, *15*, 57–74.
136. Londhe, S.N.; Shah, S.; Dixit, P.R.; Nair, T.B.; Sirisha, P.; Jain, R. A Coupled Numerical and Artificial Neural Network Model for Improving Location Specific Wave Forecast. *Appl. Ocean Res.* **2016**, *59*, 483–491.
137. Mahjoobi, J.; Etemad-Shahidi, A.; Kazeminezhad, M. Hindcasting of wave parameters using different soft computing methods. *Appl. Ocean Res.* **2008**, *30*, 28–36.
138. Etemad-Shahidi, A.; Mahjoobi, J. Comparison between M5' model tree and neural networks for prediction of significant wave height in Lake Superior. *Ocean Eng.* **2009**, *36*, 1175–1181.
139. Lin, X. ; Yang, R. ; Zhang, W. ; Zeng, N. ; Zhao, Y. ; Wang, G. ; Li, T. ; Cai, Q. An integrated view of correlated emissions of greenhouse gases and air pollutants in China. *Carbon Balance and Management.* **2023**, *18*, 9.
140. Antanasijević, D.Z.; Ristić, M.Đ.; Perić-Grujić, A.A.; Pocaajt, V.V. Forecasting GHG emissions using an optimized artificial neural network model based on correlation and principal component analysis. *Int. J. Greenh. Gas Control* **2014**, *20*, 244–253.
141. Khoshnevisan, B.; Rafiee, S.; Omid, M.; Mousazadeh, H.; Rajaeifar, M.A. Application of artificial neural networks for prediction of output energy and GHG emissions in potato production in Iran. *Agric. Syst.* **2014**, *123*, 120–127.
142. Yi, J.; Prybutok, V.R. A neural network model forecasting for prediction of daily maximum ozone concentration in an industrialized urban area. *Environ. Pollut.* **1996**, *92*, 349–357.

143. Gardner, M.W.; Dorling, S.R. Neural network modelling and prediction of hourly NO<sub>x</sub> and NO<sub>2</sub> concentrations in urban air in London. *Atmos. Environ.* **1999**, *33*, 2627–2636.
144. Jorquera, H.; Pérez, R.; Cipriano, A.; Espejo, A.; Letelier, M.V.; Acuña, G. Forecasting ozone daily maximum levels at Santiago, Chile. *Atmos. Environ.* **1998**, *32*, 3415–3424.
145. Andretta, M.; Eleuteri, A.; Fortezza, F.; Manco, D.; Mingozi, L.; Serra, R.; Tagliaferri, R. Neural networks for sulphur dioxide ground level concentrations forecasting. *Neural Comput. Appl.* **2000**, *9*, 93–100.
146. Chelani, A.B.; Rao, C.C.; Phadke, K.; Hasan, M. Prediction of sulphur dioxide concentration using artificial neural networks. *Environ. Model. Softw.* **2002**, *17*, 159–166.
147. Agirre-Basurko, E.; Ibarra-Berastegi, G.; Madariaga, I. Regression and multilayer perceptron-based models to forecast hourly O<sub>3</sub> and NO<sub>2</sub> levels in the Bilbao area. *Environ. Model. Softw.* **2006**, *21*, 430–446.
148. Elkamel, A.; Abdul-Wahab, S.; Bouhamra, W.; Alper, E. Measurement and prediction of ozone levels around a heavily industrialized area: A neural network approach. *Adv. Environ. Res.* **2001**, *5*, 47–59.
149. Antanasijević, D.Z.; Pocajt, V.V.; Povrenović, D.S.; Ristić, M.; Perić-Grujić, A.A. PM<sub>10</sub> emission forecasting using artificial neural networks and genetic algorithm input variable optimization. *Sci. Total Environ.* **2013**, *443*, 511–519.
150. Hooyberghs, J.; Mensink, C.; Dumont, G.; Fierens, F.; Bresseur, O. A neural network forecast for daily average PM<sub>10</sub> concentrations in Belgium. *Atmos. Environ.* **2005**, *39*, 3279–3289.
151. Wang, G.; Awad, O.I.; Liu, S.; Shuai, S.; Wang, Z. NO<sub>x</sub> emissions prediction based on mutual information and back propagation neural network using correlation quantitative analysis. *Energy* **2020**, *198*, 117286.
152. Babu, D.; Thangarasu, V.; Ramanathan, A. Artificial neural network approach on forecasting diesel engine characteristics fuelled with waste frying oil biodiesel. *Appl. Energy* **2020**, *263*, 114612.
153. Arcakioğlu, E.; Çelikten, I. A diesel engine's performance and exhaust emissions. *Appl. Energy* **2005**, *80*, 11–22.
154. Najafi, G.; Ghobadian, B.; Tavakoli, T.; Buttsworth, D.; Yusaf, T.; Faizollahnejad, M. Performance and exhaust emissions of a gasoline engine with ethanol blended gasoline fuels using artificial neural network. *Appl. Energy* **2009**, *86*, 630–639.
155. Sayin, C.; Ertunc, H.M.; Hosoz, M.; Kilicaslan, I.; Canakci, M. Performance and exhaust emissions of a gasoline engine using artificial neural network. *Appl. Therm. Eng.* **2007**, *27*, 46–54.
156. Shivakumar, P.; Pai, P.S.; Rao, B.S. Artificial Neural Network based prediction of performance and emission characteristics of a variable compression ratio CI engine using WCO as a biodiesel at different injection timings. *Appl. Energy* **2011**, *88*, 2344–2354.
157. Mohammadhassani, J.; Dadvand, A.; Khalilarya, S.; Solimanpur, M. Prediction and reduction of diesel engine emissions using a combined ANN-ACO method. *Appl. Soft Comput.* **2015**, *34*, 139–150.
158. Bevilacqua, V.; Intini, F.; Kühtz, S. A model of artificial neural network for the analysis of climate change. In Proceedings of the 28th International Symposium on Forecasting, Nice, France, 22–25 June 2008.
159. Bakay, M.S.; Ağbulut, Ü. Electricity production based forecasting of greenhouse gas emissions in Turkey with deep learning, support vector machine and artificial neural network algorithms. *J. Clean. Prod.* **2021**, *285*, 125324.
160. Gallo, C.; Conto, F.; Fiore, M. A Neural Network Model for Forecasting CO<sub>2</sub> Emission. *AGRIS -Line Pap. Econ. Inform.* **2014**, *6*, 31–36.
161. Abbasi, T.; Luithui, C.; Abbasi, S.A. A Model to Forecast Methane Emissions from Tropical and Subtropical Reservoirs on the Basis of Artificial Neural Networks. *Water* **2020**, *12*, 145.
162. Heo, J.S.; Kim, D.S. A new method of ozone forecasting using fuzzy expert and neural network systems. *Sci. Total Environ.* **2004**, *325*, 221–237.
163. Cai, M.; Yin, Y.; Xie, M. Prediction of hourly air pollutant concentrations near urban arterials using artificial neural network approach. *Transp. Res. Part D Transp. Environ.* **2009**, *14*, 32–41.
164. Azeez, O.S.; Pradhan, B.; Shafri, H.Z.M.; Shukla, N.; Lee, C.-W.; Rizeei, H.M. Modeling of CO Emissions from Traffic Vehicles Using Artificial Neural Networks. *Appl. Sci.* **2019**, *9*, 313.
165. Ahmadi, M.H.; Jashnani, H.; Chau, K.-W.; Kumar, R.; Rosen, M.A. Carbon dioxide emissions prediction of five Middle Eastern countries using artificial neural networks. *Energy Sources Part A Recover. Util. Environ. Eff.* **2019**, *45*, 9513–9525.
166. Nabavi-Pelesaraei, A.; Rafiee, S.; Hosseinzadeh-Bandbafha, H.; Shamshirband, S. Modeling energy consumption and greenhouse gas emissions for kiwifruit production using artificial neural networks. *J. Clean. Prod.* **2016**, *133*, 924–931.
167. Fang, D.; Zhang, X.; Yu, Q.; Jin, T.C.; Tian, L. A novel method for carbon dioxide emission forecasting based on improved Gaussian processes regression. *J. Clean. Prod.* **2018**, *173*, 143–150.
168. Stamenković, L.J.; Antanasijević, D.Z.; Ristić, M.Đ.; Perić-Grujić, A.A.; Pocajt, V.V. Prediction of nitrogen oxides emissions at the national level based on optimized artificial neural network model. *Air Qual. Atmos. Health* **2017**, *10*, 15–23.
169. Lee, W.-Y.; House, J.M.; Kyong, N.-H. Subsystem level fault diagnosis of a building's air-handling unit using general regression neural networks. *Appl. Energy* **2004**, *77*, 153–170.
170. Koziel, S.; Leifsson, L.; Couckuyt, I.; Dhaene, T. Reliable reduced cost modeling and design optimization of microwave filters using co-kriging. *Int. J. Numer. Model. Electron. Netw. Devices Fields* **2013**, *26*, 493–505.

**Disclaimer/Publisher's Note:** The statements, opinions and data contained in all publications are solely those of the individual author(s) and contributor(s) and not of MDPI and/or the editor(s). MDPI and/or the editor(s) disclaim responsibility for any injury to people or property resulting from any ideas, methods, instructions or products referred to in the content.